Contamination of surface waters by mining wastes in the Milluni Valley (Cordillera Real, Bolivia): Mineralogical and hydrological influences

Matías Miguel Salvarredy-Aranguren [a,1], Anne Probst [a,b,*], Marc Roulet [a,c,2], Marie-Pierre Isaure [d,3]

[a] *Laboratoire des Mécanismes et Transferts en Géologie (LMTG), UMR 5563, CNRS/IRD/UPS, 14 Avenue Edouard Belin, 31400 Toulouse, France*

[b] *ECOLAB UMR 5245, CNRS-INPT-Université Paul Sabatier, ENSAT Avenue de l'Agrobiopole, BP 32607 Auzeville-Tolosane, 31326 Castanet-Tolosan, Cedex, France*

[c] *Institut de Recherche pour le Développement, HYBAM, UMR 154-LMTG, CP 9214 La Paz, Bolivia*

[d] *Equipe Géochimie de l'Environnement, Laboratoire de Géophysique Interne et Tectonophysique (LGIT), UMR 5559 Université J. Fourier and CNRS, BP 53, 38041 Grenoble Cedex 9, France*

Abstract

This study is one of very few dealing with mining waste contamination in high altitude, tropical-latitude areas exploited during the last century. Geochemical, mineralogical and hydrological characterizations of potentially harmful elements (PHEs) in surface waters and sediments were performed in the Milluni Valley (main reservoir of water supply of La Paz, Bolivia, 4000 m a.s.l.), throughout different seasons during 2002–2004 to identify contamination sources and sinks, and contamination control parameters. PHE concentrations greatly exceeded the World Health Organization water guidelines for human consumption. The very acidic conditions, which resulted from the oxidation of sulfide minerals in mining waste, favoured the enrichment of dissolved PHEs ($Cd > Zn \gg As \gg Cu \sim Ni > Pb > Sn$) in surface waters downstream from the mine. Stream and lake sediments, mining waste and bedrock showed the highest PHE content in the mining area. With the exception of Fe, the PHEs were derived from specific minerals (Fe, pyrite; Zn, Cd, sphalerite, As, Fe, arsenopyrite, Cu, Fe, chalcopyrite, Pb, galena, Sn, cassiterite), but the mining was responsible for PHEs availability. Most of the PHEs were extremely mobile ($As > Fe > Pb > Cd > Zn \sim Cu > Sn$) in the mining wastes and the sediments downstream from the mine. pH and oxyhydroxides mainly explained the contrasted availability of Zn (mostly in labile fractions) and As (associated with Fe-oxyhydroxides). Unexpectedly, Pb, Zn, As, and Fe were significantly attenuated by organic matter in acidic lake sediments.

* Corresponding author. Address: ECOLAB UMR 5245, CNRS-INPT-Université Paul Sabatier, ENSAT Avenue de l'Agrobiopole, BP 32607 Auzeville-Tolosane, 31326 Castanet-Tolosan, Cedex, France. Fax: +33 5 62 19 39 01.

E-mail address: anne.probst@ensat.fr (A. Probst).

[1] Present address: Instituto de Geología y Recursos Minerales, Servicio Geológico Minero Argentino, Av. Julio A. Roca 651, 10° piso, Ciudad Autónoma de Buenos Aires 1322, Argentina.

[2] Deceased.

[3] Present address: Département de Géologie, Université de Pau et des Pays de l'Adour, Avenue de l'Université, BP 576, 64012 Pau Cedex, France.

Hydrological conditions highly influenced the behaviours of major elements and PHEs. During wet seasons, major elements were diluted by meteoric waters, whereas PHEs increased due to the dissolution of sulfides and unstable tertiary minerals that formed during dry seasons. This is particularly obvious at the beginning of the wet season and contributes to flushes of element transport downstream. The high altitude of the study area compensates for the tropical latitude, rendering the geochemical behaviour of contaminants similar to that of temperate and cold regions. These results might be representative of geochemical processes in ore deposits located in the high Andes plateau, and of their influence on PHE concentrations within the upper Amazon basin. Although mining activities in this region stopped 10 years ago, the impact of mining waste on water quality remains a serious environmental problem.

1. Introduction

Mining activities are known to be a major source of contamination (Nriagu, 1996). Movement of contaminants in and near mining sites is a complex function of the geology, hydrology, geochemistry, pedology, meteorology, microbiology, and mining and mineral processing history (Nordstrom and Alpers, 1999). At most sites, pyrite-rich ores are the main source of acid mine drainage (AMD), which may have adverse impacts on biota (Gray, 1997). Consequently, research often focuses on the complexity of biogeochemical factors involved in pyrite oxidation (Rimstidt and Vaughan, 2003; Schippers et al., 1996). Pyrite is commonly associated with several types of mineral deposits such as coal, massive sulfide and Au ores (Seal and Hammarstrom, 2003). Pyrite-rich ores in industrialised countries have been extensively investigated (Alpers et al., 2003; Audry et al., 2005; Muller et al., 2002; Sanchez España et al., 2005). However, for the last decades an important part of mining exploitation has been performed in the developing countries, where scientific investigations are less common. In South America, studies dealing with mining contamination have mainly focused on Cu and As contamination in Chile (Dittmar, 2004; Dold and Fontbote, 2002; Oyarzun et al., 2004; Romero et al., 2003; Smedley and Kinniburgh, 2002) and Hg contamination in Brasil (Lodenius and Malm, 1998; Pfeiffer et al., 1993; Wasserman et al., 2003).

Bolivia has a long mining history dating to the Spanish Colonial era (Galeano, 1971). In the last century, Bolivia became the largest producer of Sn in the world (Montes de Oca, 1982). Large and medium scale mining activities were intensively developed in several regions of the country resulting in significant environmental damage (Chatelain and Wittinton, 1992). However, few scientific studies have evaluated mining related contamination problems in Bolivia (Bervoets et al., 1998; Espi et al., 1997; Ferrari et al., 2001; Hudson-Edwards et al., 2001, 2003; Maurice-Bourgoin et al., 2003; Miller et al., 2004; Smolders et al., 2004; Oporto et al., 2007), and the geochemical behaviour at mine sites has hardly been investigated.

The Milluni Valley is located at more than 4000 m above sea level (a.s.l.) in the Bolivian Sn Belt, which is comprised of massive sulfide deposits in the Eastern Andes (Ahlfeld and Schneider-Scherbina, 1964). The Milluni Mine operated from 1940 until 1990, extracting Sn, Zn and Pb. A very large volume of sulfide-rich mine waste has been deposited in this area by different mining operations which employed a variety of separation techniques (Ríos, 1985). The only environmental studies in this area were biological investigations (Apaza Chavez, 1991; Meneses-Quisbert, 1997), which indicated important effects on biota and water quality. Since 1930, water from this catchment has drained a variety of potentially harmful elements (PHEs, Plant et al., 1997) into the main reservoir used to supply drinking water to the 1.5 million inhabitants of La Paz (Crespo, 1936). This contamination by PHEs (Fe, Mn, Zn, As, Cd, Pb, Cu, Sn) from mine waste is imprinted on this high altitude and tropical region.

The aims of this study are (i) to characterize the intensity and the sources of the mining contamination in the Milluni Valley, (ii) to determine the geochemical and mineralogical processes involved in sediment, stream and lake water contamination and, (iii) to evaluate the influence of hydrological and chemical factors on the contamination behaviour.

2. Materials and methods

2.1. Site description

The Milluni Valley, located in the high altitude Eastern Andes (locally called Royal Cordillera), is some 20 km north of La Paz. The catchment area

of ~40 km^2 constitutes part of the Altiplano basin system. Lithological units (Fig. 1) can be summarized from north to south as: (1) a granitic terrain partially covered by glaciers (Huayna Potosí granite, HPG); (2) a slightly metamorphosed fine-grained sandstone with bedded black shales (Cambrian to Ordovician); (3) a mineralized Silurian sandstone (Catavi Formation); (4) a region dominated by Quaternary till. The Catavi Formation is mainly composed of sandstone deformed

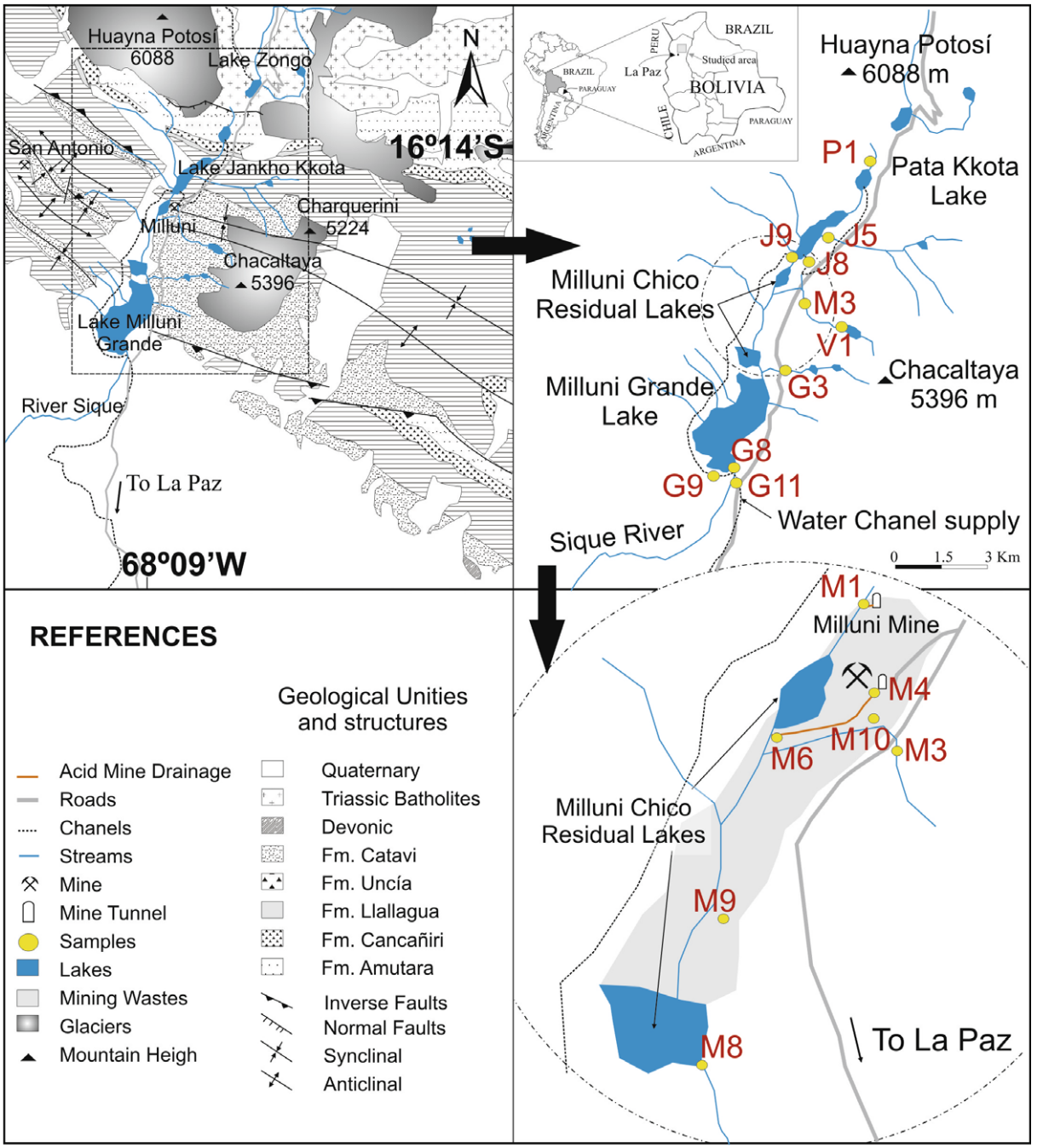

Fig. 1. Location map. On the upper right: main geological features (based on geological maps, Fernández and Thompson, 1995; Lehmann, 1978; Perez and Esktrom, 1995); on the upper left: location of the main sampling points; bottom left side: detail of the most impacted sector by mining activities.

by faults and folds, which allowed mineralisation (Ahlfeld and Schneider-Scherbina, 1964). Geological and mineralisation investigations have been performed by Lehmann (1978). The main ore minerals in the region are: pyrite (FeS_2), marcasite (FeS_2), pyrrhotite ($Fe_{1-x}S$), sphalerite (ZnS), arsenopyrite (FeAsS), cassiterite (SnO_2), galena (PbS), wolframite (Fe,Mn $[WO_4]_2$), and stannite (Cu_2FeSnS_4). Associated minerals include quartz (SiO_2), siderite ($FeCO_3$), hematite (Fe_2O_3), apatite ($Ca_5(PO_4)_3F_2$) and monazite ([Ce,La,Nd]PO_4). This mineralization was exploited underground; however, a large amount of mining waste was spread in the Milluni Chico sector (4.6 km^2) in a hazardous way on the slopes, after the minerals had been extracted by gravimetric and flotation procedures. The maximum production was during the 1970–1980s when the mine produced 1.1×10^5 Tn/a of rough mineral (Ríos, 1985).

The geomorphology of the valley has the typical U-shape and several small lakes (Fig. 1) characteristic of glacier regression (Argollo et al., 1987). These geomorphological features control drainage within the Milluni Valley. An important role of the moraines and of the sheet flow affecting the drainage has been described for the Zongo Valley and its main glacier (Caballero et al., 2002, 2004) located in the northern part of the Milluni catchment (Fig. 1). A network of diffuse runoff also was observed during the wet season in the Milluni Valley. As a consequence, extensive sampling was performed to enhance hydrochemical knowledge of the area. Several sectors of the basin, but particularly the upper basin, are draped with peat bogs and high mountain pasture land.

Even if not entirely the same, the hydrological characteristics of the Milluni basin can be considered as similar to those of the nearby Zongo area: a dry season (DS) and a wet season (WS), which occur from April to September and October to March, respectively (Fig. 2; data from SENAMHI: http://www.senamhi.gov.bo/meteorologia/climatologia.php and Great Ice IRD program; Caballero et al., 2004; Ribstein et al., 1995; Wagnon et al., 1999). Most moisture is derived from easterly winds originating in the Amazonian basin. This rainfall is greater along the main axis of the mountain (Zongo), and decreases towards the Altiplano (El Alto). Temperatures range between −6.3 and 17.4 °C with an average of 1.7 °C, but do not vary much throughout the year due to the high elevation (Ribstein et al., 1995). The bypass channel (sample G9) was built to drain the waters of Jankho Kkota Lake down the valley (Fig. 1), with the objective of avoiding the influence of the Milluni waters. A strong correlation was observed between precipitation in the region and discharge through the bypass channel (Fig. 2).

2.2. Sampling and analytical procedures

Stream sediments, mining wastes and surface waters were collected in January/February and September 2003. Additionally, certain localities (J5, M1, M3, G3, G8, G9 and partially G11) were sampled regularly (every 45 days) from January 2003

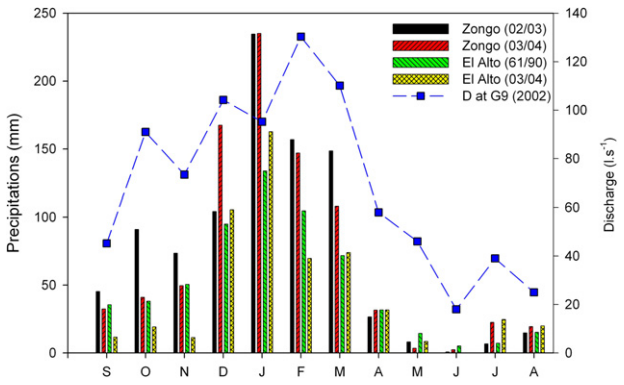

Fig. 2. Monthly precipitation for the Zongo sector during the period 2002–2003 and 2003–2004 (data from Great Ice IRD program, for more details see: Caballero et al., 2004; Ribstein et al., 1995; Wagnon et al., 1999); Mean precipitation for the period 1961–1990 and for the 2003–2004 hydrological studied year at the El Alto sector (SENAMHI: http://www.senamhi.gov.bo/meteorologia/climatologia.php); mean monthly discharge of the bypass channel (G9 sampling point) registered for the period 2002 (data from Bolivian Power Company, Gousset, A., personal communication).

until May 2004. Discharge, pH, Eh, conductivity and T (°C) were all measured *in situ*. The surface waters were filtered (<0.22 μm) according to established field protocol. One aliquot of the sample (as well as a blank) was kept for anion measurements and the rest was acidified with HNO_3 for cation and trace element analysis. After collection, samples were stored in coolers for shipment to France and not exposed to light. Suspended particulate matter was insignificant in all the samples, it was not considered in the study.

Major cations and anions were analyzed by atomic absorption spectrometry (AAS 5100 PC, Perkin–Elmer) and ion chromatography using AS-14 columns (DIONEX-DX300), respectively. The analytical results were checked using CRM BMOOS-01 (National Laboratory for Environmental Testing, 2002) and the error was consistently less than 5%. Alkalinity was determined by titration with HCl (DMS Titrino, Metrohm), the error was always less than 3%.

PHEs in sediments, mining wastes and waters were determined by ICP-MS (Elan 6000, Perkin–Elmer) using the international geostandard SLRS-4. The detection limit varied for each analysis, but generally was $<0.1\ \mu g\ l^{-1}$ for Sc, Cd, Ni, Cu, As, Sn, Mn, Ti and Pb, $<2.8\ \mu g\ l^{-1}$ for Zn and Al, and generally $<7\ \mu g\ l^{-1}$ for Fe. The analytical error was consistently less than 10%. Analytical measurements followed an interference correction for oxides and bi-charged ions according to a well-calibrated laboratory procedure (Aries et al., 2000). Results were corrected using blanks.

Sediments were air dried in a controlled atmosphere, and then sieved with Teflon-coated sieves. A portion of the <2 mm fraction was analyzed by X-ray diffraction (XRD), and the remainder was completely dissolved in strong acids ($HF/HNO_3/H_2O_2$) in a clean room. Acid digestions did not exceed 90 °C to avoid As volatilization. Every digestion was controlled with procedural blanks and certified standard sediment STDS02. Recovery of the different elements was: Zn: 109 ± 10%, As: 88 ± 9%, Sn: 107 ± 15%, Pb: 102 ± 9%, Cu: 94 ± 11%, Mn: 88 ± 11% and Fe: 83 ± 13%.

A sequential extraction procedure was performed on sediment samples. This experimental technique has been largely used in environmental studies (Filgueiras et al., 2002), and several schemes exist (Smichowski et al., 2005). The procedure of Leleyter and Probst (1999) was chosen because it has been developed for river sediments and suspended particulate matter, and tested for selectivity, reproducibility and repeatability of the different steps (for details see Leleyter and Probst, 1999; Hernandez, 2003; Leleyter et al., 1999; Brunel, 2005). This procedure is based on decreasing pH using successive reagents. At the end of the original procedure, a new step which consists of HNO_3 (5 ml, 8 N) reaction for 3 h, was added to characterize the sulfide fraction (Dold, 2003; Carlsson et al., 2002; Fanfani et al., 1997; Pagnanelli et al., 2004). The specificity of this step, essential in mining environments, was tested on a natural and near pure sample of galena, which was chosen according to its well known sensitivity to sequential extractants (Sondag, 1981). The sulfide, organic matter, Mn oxides, and acid soluble fractions represented 94.2%, 2.3%, 2.2%, and 1%, respectively, whereas the remaining phases only contained 0.3% of the Pb. It can thus be concluded that the procedure is accurate to determine the amount of element bound to the S fraction in stream sediments influenced by mining waste erosion.

XRD was performed with Co radiation (Co Kα, $\lambda = 1.789$ Å) at 40 kV for a duration of 1800 s for each sample. Scanning electronic microscopy (6360 Low Vacuum – JEOL) coupled to an energy dispersion spectrometer (SDD, Sahra Silicon Drift Detector – PGT) was used to determine minor mineralogical phases in different samples. Microprobe analysis (Cameca SX50) was applied at 15–25 kV to determine the chemical composition of the sulfide minerals.

Organic matter content was determined on 100 mg of lake sediment (G8), by thermogravimetric (TG) analysis, with a gradient of 5 °C/min up to 700 °C.

2.3. Calculations

The code WATEQ4F (Ball and Nordstrom, 1991) was used to assess the mineral saturation indices, the ion activities and the distribution of aqueous species of the surface waters.

An enrichment factor (EF) was calculated to characterize the influence of geological, hydrological and mining factors on element concentrations in surface waters (Schütz and Rahn, 1982; Shotyk, 1996). Several reference elements can be used (Zr, Hf, Ti, Al and Sc), but Zr and Hf were often below analytical detection limits, and Al was not conservative in the acidic and oxic conditions of the mining sector (Table 1). Titanium was a good candidate

Table 1
Main physico-chemical parameters and composition of water in Milluni basin

Chemical parameters, WG WHO		pH, wg						HCO_3^- (mg l^{-1}), wg						SO_4^{2-} (mg l^{-1}), 400					
Points	*n*	Wet season			Dry season			Wet season			Dry season			Wet season			Dry season		
		Min	Med	Max	Min	Med	Max	Min	Med	Max	Min	Med	Max	Min	Med	Max	Min	Med	Max
Pristine and slightly contaminated waters																			
P1	2		7.51			8.11			3.12			10.6			0.59			6.94	
J5	15	6.60	6.94	7.99	6.40	6.74	7.64	7.20	15.7	19.7	10.2	16.6	20.9	10.6	14.6	22.3	13.7	38.1	74.0
J9	2		6.68			6.61			17.0			15.7			15.5			20.6	
V1	2		4.87			4.74			1.36			1.40			28.0			25.0	
M3	17	3.69	4.04	4.35	3.81	4.27	4.65					0.60	2.56	27.9	39.5	52.9	18.0	24.5	33.7
G9	15	6.68	7.33	9.16	6.04	7.40	9.20	14.0	23.5	30.2	8.76	17.7	21.8	18.9	20.5	24.1	12.3	17.1	20.9
Highly contaminated waters																			
M1	15	2.56	2.72	2.86	2.58	3.05	3.29							897	1340.0	1550.0	757	1100.0	1630.0
M4	2		2.63			2.44									850			806	
M6	2		2.67			2.86									1060.0			7190.0	
M8	2		2.76			2.50									517			2290.0	
G3	16	2.90	3.22	3.31	2.98	3.16	3.38							99.7	124	280	90.0	138	176
G8	15	2.70	2.82	2.90	2.70	2.83	3.02							310	463	540	260	349	471

Chemical parameters, WG WHO		TDS (mg l^{-1}), wg						Ca (mg l^{-1}), wg						Mg (mg l^{-1}), wg					
Points	*n*	Wet season			Dry season			Wet season			Dry season			Wet season			Dry season		
		Min	Med	Max	Min	Med	Max	Min	Med	Max	Min	Med	Max	Min	Med	Max	Min	Med	Max
Pristine and slightly contaminated waters																			
P1	2		5.3			26.5			0.9			5.3			0.1			0.3	
J5	15	25.6	43.1	51.4	45.4	76.6	125.6	4.7	7.1	9.5	8.5	14.5	23.0	0.7	1.4	1.8	1.8	3.0	5.3
J9	2		46.2			50.6			8.6			10.0			1.4			2.2	
V1	2		43.0			36.2			3.9			3.7			3.1			2.8	
M3	17	37.5	55.3	73.8	27.5	35.4	48.3	3.5	4.1	4.7	2.7	3.2	4.4	2.4	3.3	3.9	2.0	2.3	3.2
G9	15	45.2	61.2	70.1	29.2	47.8	58.4	6.8	8.6	9.2	5.1	8.8	12.1	1.3	3.2	4.3	1.2	1.7	2.2

Highly contaminated waters																		
M1	15	1310	1940	2220	1150	1620	2290	30.3	42.9	55.5	37.4	50.9	69.2	38.0	58.9	66.8	30.6	52.1	78.8
M4	2		1220			1190			25.3			16.5			31.1			20.3	
M6	2		1480			11,000			30.2			57.8			32.1			179	
M8	2		725			3450			14.4			45.1			19.5			45.2	
G3	16	132	167	378	125	187	231	5.6	6.9	11.5	5.9	9.7	12.1	6.9	8.4	14.5	7.0	10.5	12.9
G8	15	407	643	797	379	490	634	10.5	15.1	18.0	7.2	13.3	26.8	12.3	18.8	23.0	8.8	16.9	33.9

Chemical parameters, WG WHO		Eh (mv), wg						Fe (mg l^{-1}), 0.3						Al (mg l^{-1}), 1.43					
Points	*n*	Wet season			Dry season			Wet season			Dry season			Wet season			Dry season		
		Min	Med	Max	Min	Med	Max	Min	Med	Max	Min	Med	Max	Min	Med	Max	Min	Med	Max
Pristine and slightly contaminated waters																			
P1	2		150			22			0.04			0.06			0.01			0.01	
J5	15	118	194	276	185	230	268	0.01	0.11	0.25	0.01	0.07	0.19	<0.01	0.01	0.04	<0.01	<0.01	0.01
J9	2		160			153			0.08			0.01			0.01			0.01	
V1	2		384			229			0.11			0.13			0.23			0.13	
M3	17	422	438	457	265	321	384	0.14	0.54	1.22	0.05	0.16	0.65	0.23	0.76	1.46	0.16	0.31	0.56
G9	15	129	213	308	184	293	357	0.01	0.18	0.30	0.01	0.08	0.31	0.02	0.08	0.28	<0.01	0.02	0.07
Highly contaminated waters																			
M1	15	412	420	425	319	363	407	195	367	437	152	253	310	3.0	10.5	13.9	3.6	5.4	7.4
M4	2		476			467			227			123			6.0			1.9	
M6	2		434			287			277			2900.0			21.1			24.6	
M8	2		429			362			123			905			4.5			4.4	
G3	16	476	477	480	353	434	487	4.7	7.1	11.5	7.8	14.5	21.5	1.9	3.6	13.5	0.4	1.7	3.4
G8	15	554	562	571	522	531	537	49.0	97.9	152	44.1	58.3	80.1	1.8	3.8	5.9	2.3	3.0	3.7

NB: WG WHO, water guidelines given by the World Health Organization; wg, without guideline; *n*, number of samples. If only one measurement was made, it is indicated as a median value. HCO_3^- was not measured for acid waters.

(particularly relative to hydrological discrimination), but Sc was more efficient at distinguishing between pristine and contaminated areas in terms of weathering. The EF calculated using local geochemical background or earth crust (Wedepohl, 1995) values as references, gives similar discriminations of the contaminated areas. To standardize the results, the latter was chosen:

$$\mathrm{EF} = \frac{M_w}{\mathrm{Sc}_w} \Big/ \frac{M_{ec}}{\mathrm{Sc}_{ec}} \quad (1)$$

where EF is enrichment factor, M is the PHE of interest, Sc is scandium, and subscript w indicated surface water concentration and ec earth crust concentration. An EF between 0.5 and 2 is in the range of natural variability, whereas values greater than 2 indicate a likelihood of anthropogenic enrichment (Hernandez et al., 2003; Schütz and Rahn, 1982).

3. Results

3.1. Chemical composition of surface waters

3.1.1. Major elements

Table 1 presents physical and chemical parameters for representative surface water samples. Pristine waters originate from separate geochemical formations: a granitic area (P1) and a non-mined mineralized unit (Catavi Formation, V1). The pH and TDS values indicate a clear difference between pristine or slightly contaminated and mining impacted waters. This shift in aqueous geochemistry was observed for all cations. Water from the mining sector is characterized by a decrease in pH and alkalinity and an increase in SO_4^{2-} concentrations.

Piper diagrams were used to compare major ion composition of WS water samples, which exhibited large variations in TDS (Fig. 3). Cation (Fig. 3a) and anion (Fig. 3b) distributions identify three regions with distinct water compositions: (1) the upper basin, including the Pata Kkota sector (PK, black circles), dominated by Ca^{2+} and HCO_3^-; (2) the middle basin, in the vicinity of Jankho Kkota (JK, black squares) with a transition from Ca^{2+} and HCO_3^- to $Ca^{2+} + Mg^{2+}$ and $HCO_3^- + SO_4^{2-}$ dominated waters; (3) the mining and downstream region including the Milluni Chico (MC) and Milluni Grande (MG) areas (triangles), which is characterized by SO_4^{2-} plus a range between nearly equal proportions of Ca^{2+} and Mg^{2+}, to Mg^{2+} dominated waters.

Whatever the season, the Eh of surface waters was higher in mine outputs (M1, M4) than in pristine waters (P1, V1). There was a general trend of decreasing Eh value from WS to DS in all catchments, however, all values were indicative of oxidizing conditions. Most of the chemical species in the highly contaminated waters exceeded the water guidelines proposed by the World Health Organization (WG WHO, O.P.S., 1987, Table 1).

3.1.2. PHEs

PHE concentrations in the Milluni waters (Table 2) shows a huge break between waters draining the pristine and slightly contaminated areas and those draining the mining area. A generally decreasing trend in concentrations was observed for contaminated waters (Tables 1 and 2), with five orders of magnitude difference between Fe and Pb: $Fe \gg Zn > Mn \sim Al \gg As \sim Cu > Cd \gg Pb$. This

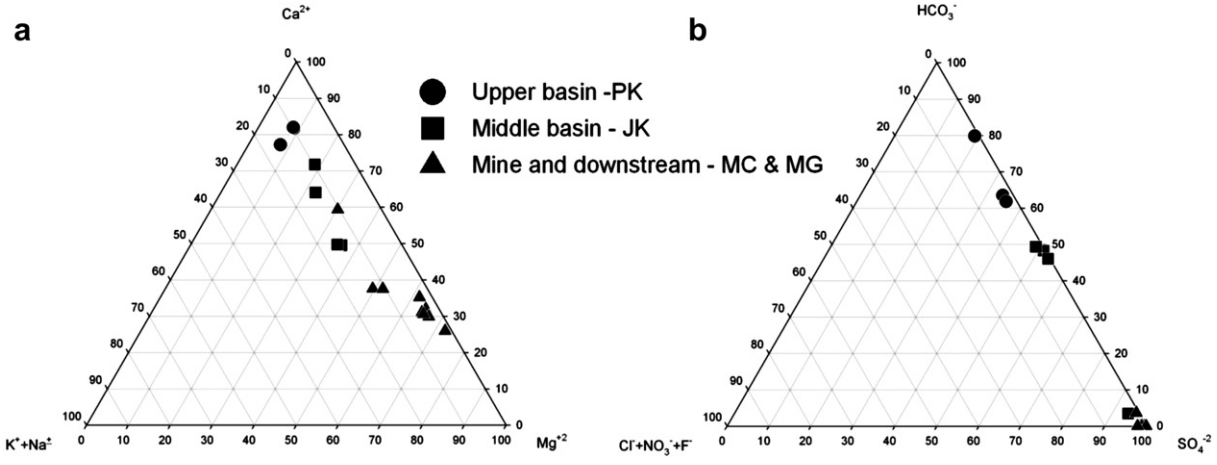

Fig. 3. Piper diagrams for cations (a) and anions (b) of the main streams from the Milluni Valley during the wet season.

Table 2
PHE concentrations in waters of Milluni Valley

Chemical parameters, WG WHO		Zn (μg l^{-1}), 2000						Mn (μg l^{-1}), 500						As (μg l^{-1}), 10					
Points	*n*	Wet season			Dry season			Wet season			Dry season			Wet season			Dry season		
		Min	Med	Max	Min	Med	Max	Min	Med	Max	Min	Med	Max	Min	Med	Max	Min	Med	Max
Pristine and slightly contaminated waters																			
P1	2		13.4			0.5			6.4			8.3			3.7			4.4	
J5	15	32.6	129.0	206	81.7	261	425	48.5	214	330	4.6	76.8	175	0.7	1.0	1.5	0.1	0.4	0.9
J9	2		58.8			49.3			51.4			13.5			2.3			0.6	
V1	2		1080			756			336			305			0.5			0.4	
M3	17	1230	2110	3170	810	1180	1530	557	625	778	274	426	548	0.8	1.5	2.2	0.5	0.9	2.1
G9	15	16.8	101	220	10.0	110	282	13.4	88.6	125	<0.1	43.1	160	1.1	1.9	3.0	0.5	1.5	3.2
Highly contaminated waters																			
M1	15	55,100	74,200	119,000	78,600	126,000	166,000	17,500	28,400	33,500	14.5	27.2	35.2	23	1180	2280	40	115	232
M4	2		53,800			202,000			14,000			11.6			3560			573	
M6	2		28,100			489,000			15,500			105			4600			17,800	
M8	2		26,700			114,000			9350			25.6			636			1400	
G3	16	2580	6890	25,800	2090	4610	8840	1200	2530	12,200	1.0	2.1	4.5	6.2	24	121	3.6	16	37
G8	15	16,100	29,000	57,200	22,400	31,400	39,800	3860	8420	13,200	5.5	7.2	9.2	19	77	170	16	29	37

Chemical parameters, WG WHO		Cu (μg l^{-1}), 1300						Cd (μg l^{-1}), 3						Pb (μg l^{-1}), 10					
Points	*n*	Wet season			Dry season			Wet season			Dry season			Wet season			Dry season		
		Min	Med	Max	Min	Med	Max	Min	Med	Max	Min	Med	Max	Min	Med	Max	Min	Med	Max
Pristine and slightly contaminated waters																			
P1	2		0.7			0.2			<0.1			<0.1			0.1			<0.1	
J5	15	<0.1	0.5	1.1	0.1	0.3	0.5	<0.1	0.2	0.3	0.2	0.3	0.6	<0.1	0.1	0.3	<0.1	<0.1	0.3
J9	2		3.3			0.9			0.1			0.2			19.0			<0.1	
V1	2		51.7			31.1			3.6			2.5			0.2			<0.1	

(*continued on next page*)

Table 2 (*continued*)

Chemical parameters, WG WHO		Cu (μg l^{-1}), 1300						Cd (μg l^{-1}), 3						Pb (μg l^{-1}), 10					
Points	*n*	Wet season			Dry season			Wet season			Dry season			Wet season			Dry season		
		Min	Med	Max	Min	Med	Max	Min	Med	Max	Min	Med	Max	Min	Med	Max	Min	Med	Max
M3	17	49.5	85.5	129	37.4	60.2	92.3	4.6	9.8	15.4	3.4	5.2	7.6	1.5	3.9	10.9	0.7	2.4	3.8
G9	15	0.4	2.6	4.4	1.0	2.7	4.4	<0.1	0.3	0.5	<0.1	0.3	0.6	<0.1	0.3	0.9	<0.1	0.1	0.4
Highly contaminated waters																			
M1	15	311	1870	2560	496	1160	1700	217	734	1010	315	441	590	5.3	22	36	3.8	8.1	13
M4	2		1520			2050			862			602			82			90	
M6	2		1550			993			280			243			21			7.2	
M8	2		877			477			185			225			17			8.2	
G3	16	62	139	371	8.0	57	119	9.2	19	46	1.8	7.7	12	24	74	283	4.3	33	80
G8	15	276	511	766	344	516	649	47	103	167	76	99	127	5.9	15	24	5.5	9.5	12

NB: WG WHO, water guidelines given by the World Health Organization; *n*, number of samples.

trend was similar for pristine and slightly contaminated waters, but the difference between Fe and Pb concentrations was only three orders of magnitude. PHE speciation calculated for contaminated waters showed that >60% of Zn, Cd, Cu, Ni, Fe and Mn were as free cations and the remaining fraction was represented mostly by SO_4 complexes. Only Pb was dominated by SO_4 complexes (~60%). Arsenic was mainly as $H_2AsO_4^{1-}$ (>70%).

Cadmium was the only element for which guidelines proposed by WHO (Table 2), were exceeded in the background area (V1) during the WS. In slightly contaminated waters (M3, J9), during the WS the guidelines for Zn, Mn and Cd in M3 and Pb in J9, also were exceeded. Most of the PHEs in highly contaminated waters greatly exceeded the water guidelines, whereas at the outlet of the system (G8), only Zn, Mn, As, Cd and Pb did.

A seasonal comparison of PHE concentrations in surface waters reveals a significant hydrological influence (Table 2). This seasonal variation of PHEs is clearly observed at the mine output (M1, Fig. 4). In general, As and other PHEs (Pb, and to a lesser extend Cu and Cd) concentrations increased during the WS, with the exception of Zn in highly contaminated waters, which increased during DS.

Average concentrations of PHEs (Zn, Mn, As, Cd, Cu, Pb, Table 2) in the mining sector (M1, M4, M6, Fig. 1) were at least one order of magnitude higher than in the pristine areas. Downstream, in Milluni Grande Lake (G8), PHE concentrations decreased substantially, however, they remained at least seven times to several orders of magnitude higher than in pristine waters (P1, V1, particularly As, Zn and Mn).

3.2. Mineralogical composition of sediments and mining wastes

Field observations (Fig. 5), XRD analysis of 45 bed sediment samples (fraction <2 mm, Table 3) and SEM–EDS investigations revealed the variation of mineralogical composition within the valley. Sediments from Pata Kkota and Jankho Kkota sectors (upper valley) are characterized by primary silicate minerals. In the mining sector, primary sulfide minerals dominated (Milluni Chico sector, Figs. 1 and 5a: dark sediments bordered by white line).

Enriched sulfide mining wastes (M10) were mainly composed of pyrite and sphalerite, but chalcopyrite and arsenopyrite also were common (Fig. 6). Fresh mining waste also contained tertiary

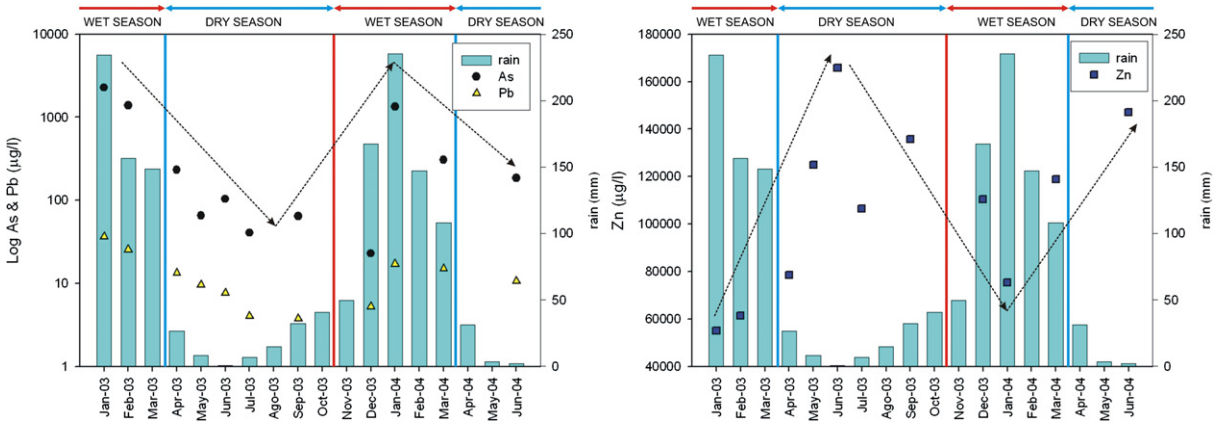

Fig. 4. Seasonal variations of As, Pb and Zn concentrations at the output of the Milluni Mine (M1), and amount of precipitation during the year. Arsenic and Pb increased during the wet season, conversely Zn decreased during this season. Rain data from Great Ice IRD program.

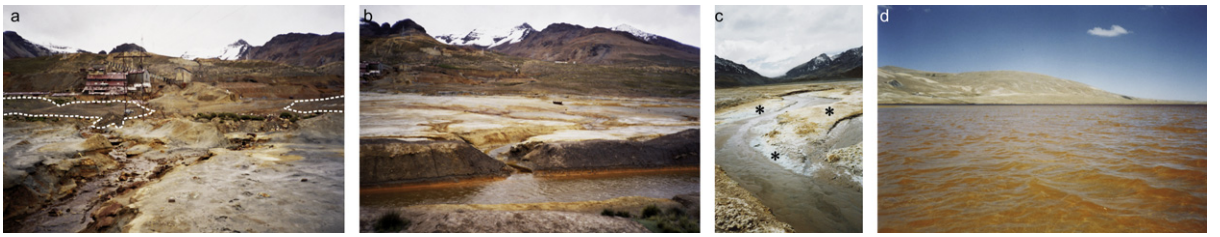

Fig. 5. Photographs of the different sampling sites of sediments and mining wastes in Milluni Chico and Milluni Grande. Photograph locations are shown on Fig. 1: (a) Milluni Mine, white lines show dark mining wastes rich in sulfides; (b) weathered mining wastes in the Milluni Chico sector; (c) efflorescent tertiary minerals in Milluni Chico during the dry season indicated by the asterisks; and (d) orange waters and sediments very rich in Fe-oxyhydroxides in Milluni Grande Lake.

minerals, such as jarosite. The appearance of these minerals ranges from dark stains in primary minerals to completely altered grains and they contain elevated concentrations of PHEs, especially As. SEM and EDS images (Fig. 7) revealed the presence of other minerals such as complex Pb sulfates or bismuthinite (Bi_2S_3), and confirmed the occurrence of cassiterite (SnO_2). Although the features of sulfide mineral alteration products seemed homogenous (Fig. 7a, secondary electron image) their chemistry and mineralogical composition might be relatively complex (Fig. 7b, backscattered electron composition). Fig. 7b shows small pyrite grains within Pb sulfate, and in some locations elemental S (circled and marked by "S"). Some primary sulfide minerals, such as bismuthinite (Fig. 7c) appeared unoxidized, but the mineral boundaries were irregular. On the order hand, primary oxides such as cassiterite (Fig. 7d), zircon and quartz showed no evidence of weathering. Even though neighbouring phyllosilicates and quartz are fully preserved, monazite crystals have diffuse borders and altered surfaces (Fig. 7e).

In the main channel linking the Milluni Chico residual lakes (M2, Fig. 1), Fe-oxyhydroxides and sulfates (amorphous, jarosite and goethite), which are products of intense chemical weathering, dominated (Fig. 5b). These sediments contained a mixture of sulfides and Fe-oxyhydroxides (Fig. 7f) as well as intimate mixing of oxidized pyrite, illite and goethite (Fig. 7g). In the highly weathered mining wastes deposited in the central sector of Milluni Chico (M6, Fig. 5b), Fe-oxyhydroxides dominated and commonly cover other mineral grains (Fig. 7h). Sulfides also are present, but they have been intensively altered by oxidation (Fig. 7i). Finally, during the DS in distal mining wastes (M9), efflorescent minerals were observed (Table 3, Figs. 7j and 5c), such as melanterite.

The mineralogy of sediments from the Milluni Grande sector (downstream) was dominated by Fe-oxyhydroxides, in addition to recalcitrant

Table 3
Synthetic mineralogical composition of bed sediments and tailings from the Milluni basin

Type	Basin sector, sample	Upper basin		Mining sector			Lower basin		
		Pata Kkota and Jankho Kkota streams sediments (PK–JK)	Catavi background (Ventanani)	Fresh tailing mine	Neoformation minerals in distal tailings	Lixiviated tailings	Mining activity (material rock extraction)	Milluni Grande L. bottom sediments	Output channel
Minerals									
Primary	Quartz	(+++)	(+++)	(++)		(+++)	(+++)	(+++)	(+++)
	Orthoclase	(++)							
	Muscovite	(++)	(++)				(++)	(++)	(++)
	Albite	(+)				(++)			(++)
	Microcline	(+)							(+)
	Anorthite	(+)							
	Cassiterite			(+)					
	Sphalerite			(++)	(+)				
	Pyrite			(+++)	(+)	(t)			
Secondary	Siderite			(t)					
	Chlorite	(+)	(+)			(+)		(+)	(+)
Tertiary	Rozenite				(+++)				
	Melanterite				(+++)				
	Diaspore				(+)				
	Jarosite					(+)			
	Goethite						(+)		
	Fe-oxyhydroxides						(+)	(+)	(+)
Accesory	Anastase								(+-t)

Three main areas of the valley were discerned: the upper part (PK, JK, V sectors), the mining sector (Milluni Chico sector) and the lower part (Milluni Grande sector).

primary silicate minerals and accessory phases (Table 3). A similar mineralogic composition was observed for Milluni Grande Lake bottom sediments (G8, Figs. 1 and 5d), which are mainly composed of a complex mixture of Fe-oxyhydroxides and silicates (Fig. 7k and l).

3.3. Chemical composition of sediment and mining wastes

3.3.1. Mineral phases

The chemical composition of the different sulfide minerals from the Milluni Chico sector (M2, M6, M9 and M10) was investigated by microprobe analyses (Table 4). The samples commonly contained pyrite and sphalerite, and more rarely chalcopyrite and arsenopyrite. Conversely, sulfides such as stannite or kesterite as expected were uncommon, as cassiterite, which is a primary oxide, is the main Sn ore mineral.

Arsenopyrite was the main As source, whereas pyrite content was very low. Chalcopyrite was the major Cu bearing mineral, but kesterite ($Cu_2(Zn,Fe)SnS_4$), stannite (Cu_2FeSnS_4) and sphalerite are secondary sources. Kesterite and stannite are Sn sulfides, but also may contain Cu, Fe and Zn. Pyrite was the main source of Fe, although Fe also was present in other primary minerals. Sphalerite was the primary source of Zn and Cd, however, kesterite also may contain trace amounts of Cd. Sulfur was associated with pyrite, chalcopyrite and sphalerite, while other sulfides contained only half of the pyrite S concentration. Lead, Ni and Co were not detected.

3.3.2. Bulk element concentration

Total bulk PHE concentrations for sediments, mining waste and bedrock, as well as sediment guidelines (Ingersoll et al., 2000) are shown in Table 5. Measured Eh values suggest that streams and lake bed sediments are oxidizing environments. The pH of sediments affected by mining was very low, with values close to the corresponding surface waters (Table 2). The fresh mining wastes (M10)

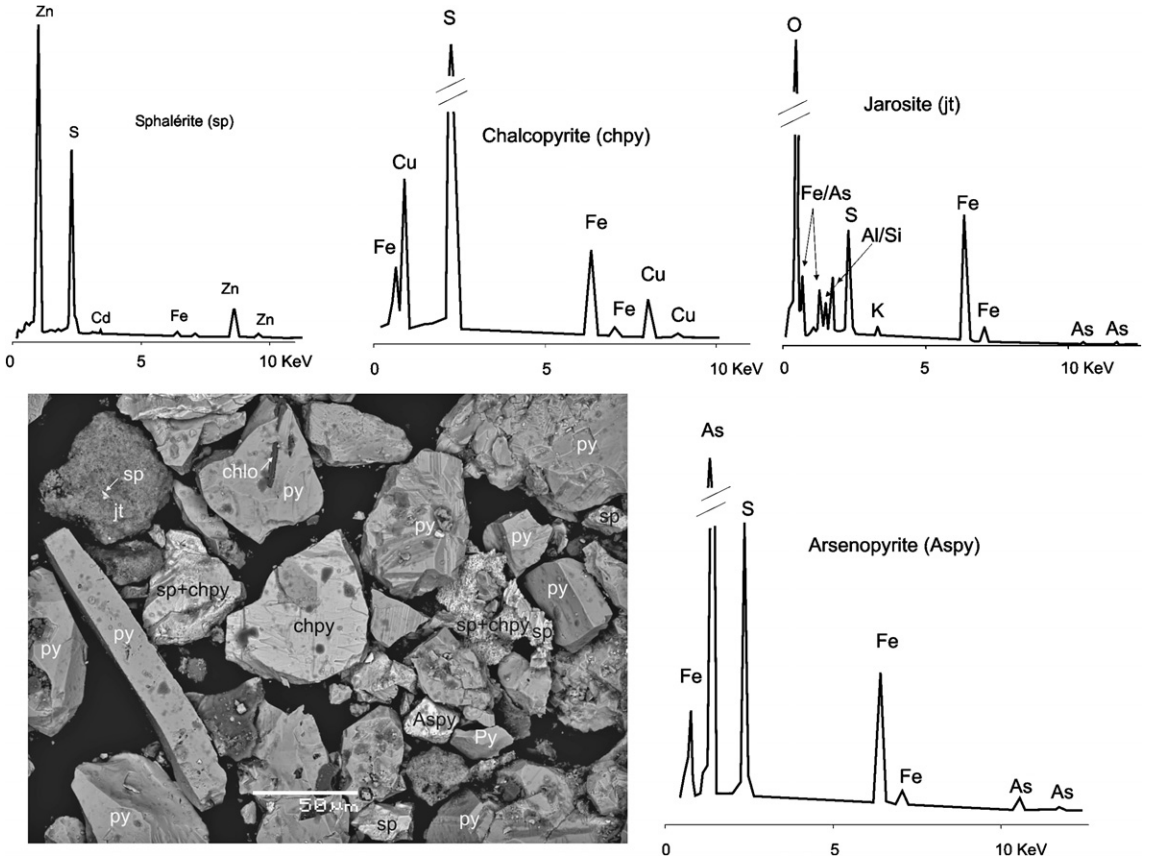

Fig. 6. Enriched mining waste sulfides from Milluni Mine (M10) as shown by backscattered electron microscopy. Semi-quantitative chemistry was defined by EDS spectra.

had the highest concentrations, with the exception of Mn and Pb. The highest Mn and Pb concentrations in the region were found in a sample of bedrock waste from the ore. Arsenic concentrations were clearly higher in mining-affected sediments and wastes than in bedrock from the different geological units. Zinc concentrations in bedrocks and sediments, including some background sediments (e.g. V1), were often higher than sediment guideline values. The same pattern was observed for Mn, As and Sn, for which sediments from pristine areas (i.e. P1, P2, V1) exceeded their respective guidelines. On the other hand, Cu, Cd and Pb guidelines were only exceeded in mining-affected samples. Iron was present at high concentrations in pyrite-rich mining wastes, and in oxide-rich sediments.

3.3.3. Distribution of PHEs between residual and non-residual fractions

Sequential extractions were performed on three typical samples of the different types of sedimentological conditions found in the area (Fig. 8): (i) sediment representing geochemical background (P1), (ii) mining wastes (M10), and (iii) sediment close to the outlet of the Milluni Grande Lake (G8), with the aim of determining where PHEs reside.

Zinc was dispersed among the different phases, particularly in the background sample (P1, Fig. 8). Downstream, samples M10 and G8 showed a significant increase of water-leachable Zn. In mining wastes (M10), Zn was mainly bound to sulfides, whereas it was mainly found in the residue and in the organic fraction in the lake sediments (G8).

In general Fe oxides (Fig. 8) were the main As residence, particularly amorphous Fe oxides in the background area (P1), but also in M10 sample where the major As source was sulfides. On the other hand, in G8, As was primarily associated with crystalline Fe oxides and to a lesser extent organic matter.

Lead was primarily associated with organic matter (Fig. 8), but the residual phase was also important in P1. In M10, Pb was bound to organic

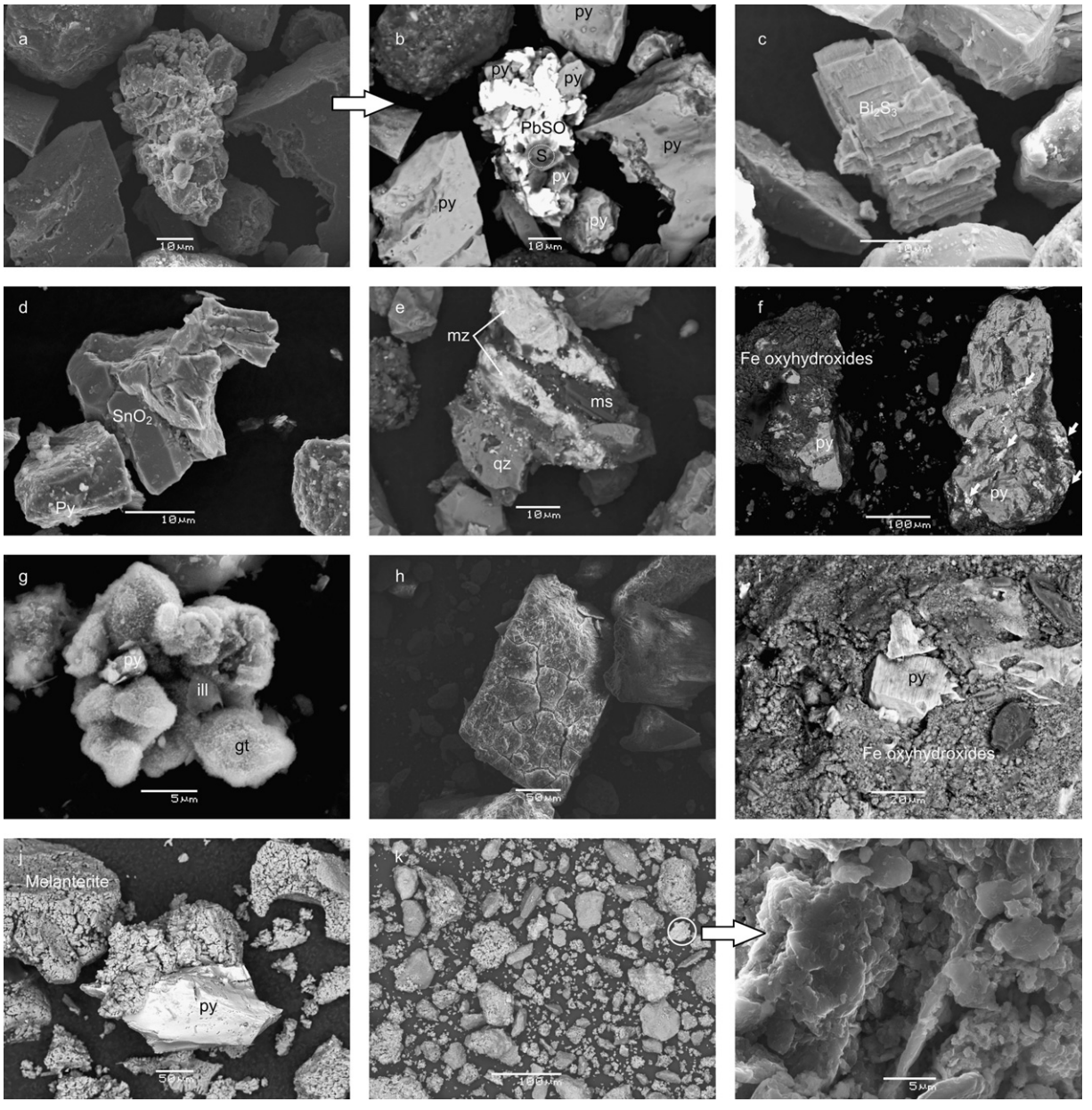

Fig. 7. Secondary electron (SEI), backscattered electron composition (BEC) and backscattered electron shadow (BES) images: (a) lead complexed sulfate in M10 (SEI); (b) same image as "a", but in BEC defining: pyrite (py), pure S (S), lead sulfate ($PbSO_4$); (c) bismuthinite (Bi_2S_3) in M10 (BEC); (d) cassiterite (SnO_2) in M10 (BEC); (e) monazite (mz), quartz (qz) and muscovite (ms) in M10 (BEC); (f) on the right: Fe-oxyhydroxides surrounding py, on the left: white arrows show cassiterite inclusions in py in M2 (BEC); (g) Close mixing of oxidized py, illite clay sheet (ill) and goethite (gt) in M2 (SEI, partial vacuum); (h) Fe-oxyhydroxides covering grains in M6 (SEI); (i) very altered py remaining in Fe-oxyhydroxide mass in M6 (BES); (j) precipitated sulfate (melanterite) during the dry season, mixed with residual py in M9 (BEC); (k) silicates mixed with inseparable mix of phyllosilicates (probably illite) and Fe-oxyhydroxides in G8 (BEC); (l) detail of inseparable mix of phyllosilicates (probably illite) and Fe-oxyhydroxides in G8 (SEI).

matter and sulfides, however, oxides played an important role as well. Finally, the organic fraction played a major role in lake sediments (G8) with crystallized oxides and residual phases.

Iron exhibited a distinct pattern for each sample (Fig. 8). Iron in sample P1 distributed among the various fractions, whereas it was primarily associated with sulfides in mining wastes. In sample G8,

Table 4
Average sulfide mineral compositions given by microprobe analyses in mining wastes from Milluni Chico sector

Mineral name	Elements in % (1% = 10,000 mg kg^{-1})							Recovery (%)
	S	Fe	Zn	As	Cu	Sn	Cd	
Arsenopyrite	20.2	34.4	<dl	44.8	<dl	<dl	<dl	99.8
Chalcopyrite	34.9	29.2	1.7	<dl	33.6	<dl	<dl	99.5
Kesterite	28.8	10.1	3.2	<dl	29.2	27.0	0.1	98.5
Pyrite	52.0	46.5	<dl	0.4	<dl	<dl	<dl	99.0
Sphalerite	33.5	6.3	56.1	<dl	4.1	<dl	0.2	100.3

NB: Detection limits were 362 for S; 417 for Fe, 589 for Cu, 754 for Cd, 850 for As, 675 for Zn and 763 mg kg^{-1} for Sn; <dl = under detection limit.

Fe was bound to both amorphous and crystalline Fe oxides, but organic matter also played a significant role.

Tin was primarily bound to the mineral lattice (Fig. 8). However, sulfides also played an important role in mining wastes and crystalline oxides did in G8.

3.3.4. Organic content in Milluni Grande Lake

Sequential extractions indicated that elements were bound to organic matter (OM) to a certain extent in lake sediments (G8). Even though the method from Leleyter and Probst (1999) was developed for river sediments and was somewhat constrained regarding the fraction selectivity, this result was unexpected. To verify that this result was realistic, OM content was determined, and indicated that this sediment (G8) contains 5.5%. This OM might originate in the numerous peat bogs from the upper basin. No data on OM content was available for P1 and M10.

4. Discussion

4.1. Mineralogical sources and sinks and availability of PHEs in the Milluni Valley

Sediments and mining wastes were investigated to identify potential sources and sinks of PHEs and to evaluate the extent of contamination. The mineralogy and geology of the area account for most of the observed variation in bulk concentration of PHEs in sediments and mining wastes, with the highest PHE contents observed in samples from the mining sector (Table 5). Nevertheless, the PHE mobility in the environment was enhanced by mining operations (Tables 1, 2 and 5). As indicated by XRD, SEM & EDS analysis, sulfides were identified as a principal source of PHEs in the Milluni catchment, although primary oxides also might be important with respect to elements such as Sn. Most of the PHEs were mineral specific; only Fe originated from multiple minerals, as determined by microprobe analysis (Table 4). Nevertheless, pyrite was the main source of Fe owing to its abundance.

4.1.1. As

Arsenic concentrations in the background areas and in bedrocks of different geological units were low in comparison to contaminated sediments and mining wastes (Table 5). Mining exploitation had the greatest influence on As concentration in sediments. This undesirable by-product of mining activity results from the oxidative weathering of arsenopyrite. However, As concentrations in contaminated sediments and mining wastes depended on sample mineralogy. Only in fresh mining wastes were sulfides a significant mineralogical source of As (M10, Figs. 6 and 8). In general, As was preferentially associated with Fe-oxyhydroxides (e.g. ~0.7 % of As in contaminated sediments enriched in Fe-oxyhydroxides, J8, Table 5), which are well-known to scavenge As and thus constitute an important sink and a temporary control on contamination (Carlson et al., 2002; Filippi, 2004; Garcia-Sanchez and Alvarez-Ayuso, 2003; Savage et al., 2005; Smedley and Kinniburgh, 2002). pH is a key parameter for the stability of the Fe-oxyhydroxide minerals. Hence, jarosite was found only in sediments in most acidic waters (M1, M6) and not in areas with pH > 3 (Baron and Palmer, 1996; Gasharova et al., 2005). Bigham et al. (1996) pointed out that schwermannite precipitates over a pH range of 2.8–4.5, associated with jarosite or goethite. Indeed, it was found that jarosite and schwermannite precipitated together in a non-acidified water sample (M6) after 6 months of storage in the laboratory (Fig. 9).

Even though physical and chemical parameters play an important role in As mobility and availability among solid-liquid phases, diagenesis might be

Table 5
pH, Eh and bulk chemical composition of the bed sediments, mining wastes and bedrocks from the Milluni Valley

Element, SG EPA	Fe (%)		Zn (mg kg^{-1}), 410		Mn (mg kg^{-1}), 260		As (mg kg^{-1}), 70		Cu (mg kg^{-1}), 270		Cd (mg kg^{-1}), 9.6		Pb (mg kg^{-1}), 218		Sn (mg kg^{-1}), 3.4		pH, wg	Eh (mv), wg
	Conc	SD (%)	Conc	SD (%)	Conc	SD (%)	Conc	SD (%)	Conc	SD (%)	Conc	SD (%)	Conc	SD (%)	Conc	SD (%)		
Bed sediments																		
P1	nd	nd	252	2.7	983	3.4	220	2.2	14	3.1	0.9	8.7	44	5.5	9.4	4.9	nd	nd
P2	nd	nd	83	2.8	nd	nd	99	2.8	4	2.9	0.2	6.3	32	3.8	5.4	3.3	nd	nd
J5	nd	nd	368	2.9	715	3.2	56	2.8	20	3.8	1.5	7.3	30	6.1	5.1	11.4	6.5	240
J8	nd	nd	868	2.5	97	3.5	6860	2.4	105	3.2	1.0	8.6	349	4.3	4.5	8.8	4.8	380
V1	nd	nd	1490	2.8	850	3.4	90	2.2	161	2.8	3.0	3.1	62	4.5	23.9	2.8	5.2	330
M2	nd	nd	8300	2.5	1360	2.9	3410	2.2	562	2.9	39.3	3.1	160	4.1	152	22.5	3.4	290
M3	nd	nd	229	3.1	nd	nd	1170	3.0	52	2.9	1.0	5.0	197	3.6	68.9	3.4	3.7	370
M6	10.6	1.2	788	6.0	841	4.0	2900	1.1	149	5.7	2.2	6.6	244	6.2	400	15.0	nd	nd
M8	nd	nd	499	2.7	172	2.9	3120	2.4	194	3.1	1.6	8.1	1400	4.4	1085	11.9	3.2	450
M9	17.4	6.1	12,100	4.0	2120	4.6	844	6.6	131	17.0	5.1	8.4	53	2.8	244	21.0	–	–
M10	31.6	4.9	26,700	2.0	77	0.7	5600	0.5	3550	3.5	118	2.5	846	0.4	2000.0	3.4	3.0	290
G3	29.6	2.9	979	2.7	110	2.7	4030	2.5	242	2.7	0.9	8.7	671	8.1	656	6.5	3.6	500
G8	18.1	6.2	403	3.8	164	5.7	1030	4.0	79	5.5	1.6	8.2	61	4.9	30.7	17.6	2.3	380
G11	11.3	3.0	309	4.0	272	2.8	234	2.7	53	2.8	0.6	17.0	37	3.9	8.6	3.4	nd	nd
Geological units																		
HPG	nd	nd	1490	2.8	357	3.3	90	2.2	9	4.1	0.6	11.9	33	4.9	11.4	3.2	–	–
Fm Uncia	nd	nd	134	2.8	321	2.7	17	2.8	19	3.4	0.3	14.8	14	5.3	4.3	8.7	–	–
Fm Catavi	nd	nd	1950	2.4	84	2.9	269	2.1	60	3.1	6.3	4.6	174	4.6	nd	nd	–	–
Rock waste ore	nd	nd	1560	2.7	7980	3.5	389	2.6	1750	3.0	5.8	6.2	2680	4.2	730	3.0	–	–

NB: SG EPA: sediment guidelines values given by the Environmental Protection Agency (Ingersoll et al., 2000); wg: without guidelines; Conc: concentration; nd: not determined; –: not relevant, HPG: Huayna Potosí granite. For the different sampling sites, see Fig. 1.

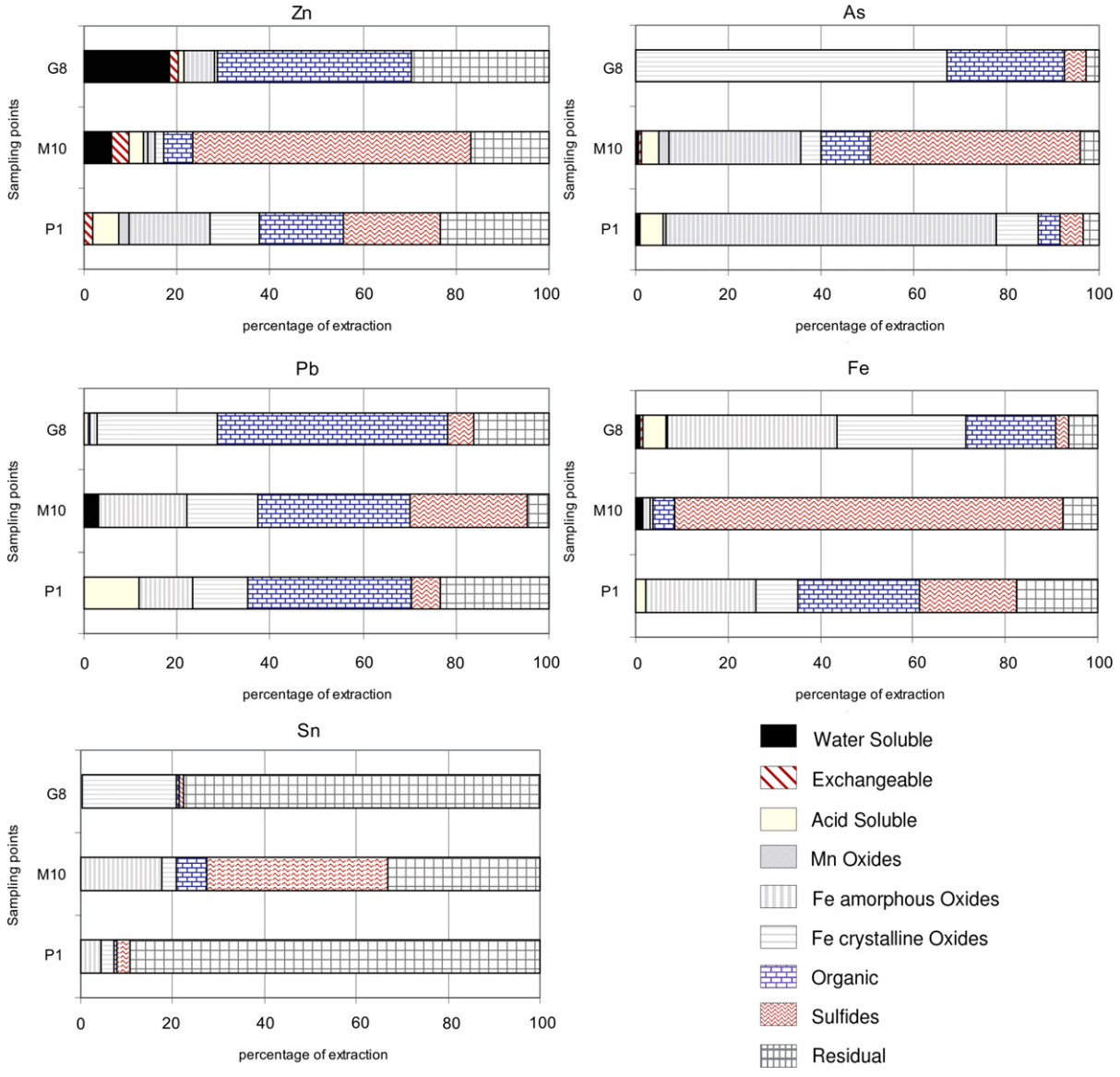

Fig. 8. Percentages of Zn, As, Pb, Fe and Sn associated with different phases determined by the sequential extraction procedure (Leleyter and Probst, 1999, modified) in three samples of sediments from the Milluni Valley.

another important controlling factor (Courtin-Nomade et al., 2003), as amorphous and disordered structures such as Fe-oxyhydroxides evolve towards more ordered crystalline structures such as goethite (Cornell and Schwertmann, 1996). This probably explains why goethite was found, even at low pH, in the acid lakes of Milluni Valley (pH $\sim$ 3, M8, G8). The sequential extraction performed on the sediment outlet of the system (G8), showed that As was mostly associated with the crystalline oxides, in agreement with mineralogical observations (XRD). Iron-oxyhydroxide diagenesis has been suggested as a secondary As source (Courtin-Nomade et al., 2003).

The combination of mineralogical (EDS/SEM and XRD) and chemical (sequential extractions) investigations argues for the retention of As in the Fe-oxyhydroxide fraction. Nevertheless, the sequential extraction of lake sediments (G8) reveals a significant portion of As bound to OM, which was rather unexpected in this acid-oxic environment, but the OM content measured in this sediment is

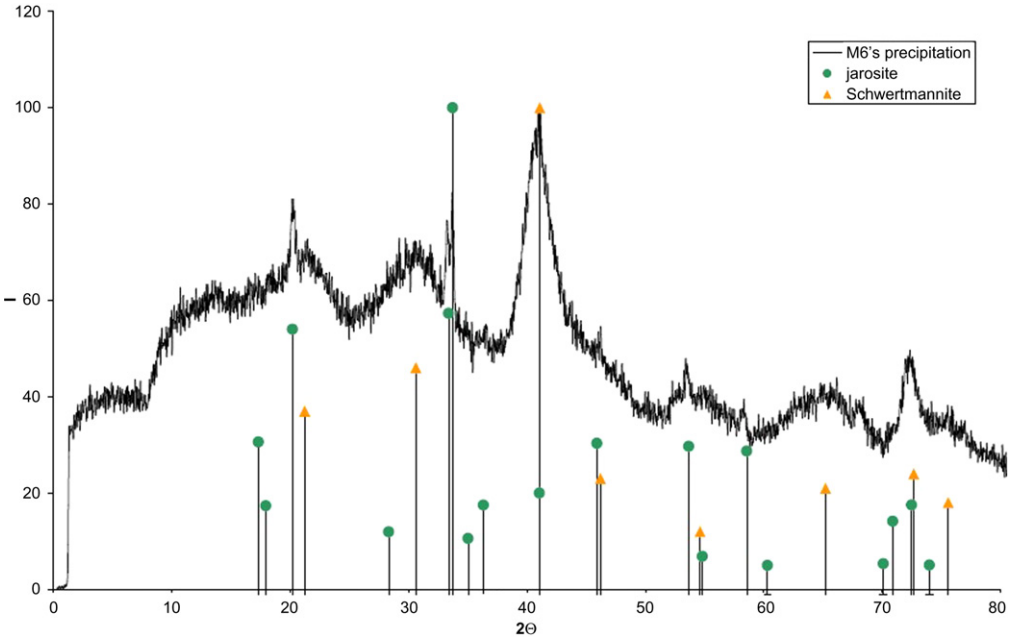

Fig. 9. XRD spectrum of the precipitated fraction in the non-acidified M6 water sample (after 6 months storage). Mineralogical patterns of jarosite and schwertmannite are indicated by circles and triangles, respectively.

consistent with such an interpretation (Section 3.3.4).

4.1.2. Cd and Zn

Sphalerite was the main source of Zn and Cd, which is a trace element in sphalerite (Wedepohl, 1995). Cadmium concentrations in sediments were generally very low; however, Cd is highly toxic even at low concentrations. As with As, the mining process has a strong influence on Cd concentrations in samples from the mining area (M2, M10, Table 5), which were very high compared with samples from the Catavi Formation or the waste rock. In Milluni Grande sediments (G8), Cd normalizated to Ti was more enriched than recent lacustrine sediment values as proposed by Callender (2003). This argues for Cd transfer downstream in the Milluni valley in relation to its high solubility under acidic conditions such as in the mining area (Callender, 2003; Gomez Ariza et al., 2000; Licheng and Guijiu, 1996). In fresh mining wastes (M10), Cd was mainly linked to sulphides (according to mineralogical analysis and sequential extraction – data not shown). The most labile mineralogical fractions accounted for around 14% of Cd in this sample; probably a product of alteration of sphalerite (Fig. 6). Whereas, in the background and outlet Milluni lake samples (P1, G8), the non-residual fractions represent around 30% of Cd, verifying the high availability of this element (Licheng and Guijiu, 1996; Morillo et al., 2002). Downstream from the mine (G8), 24% of Cd in sediments was leached with water, which likely indicates greater bioavailability (Galay Burgos and Rainbow, 2001). The high solubility of Cd allowed transitory storage in tertiary minerals (Alpers et al., 2003) such as melanterite, which precipitated in distal fine tailings (M9, Figs. 5c and 7j and Table 5) during DS.

Even if Cd and Zn originated from the same mineral source, they did not behave in the same way throughout the drainage basin. The exception was in fresh mining waste (M10) and in precipitated sulfates (M9), which can be considered as end-members in the weathering process. In samples where mineralogical composition was more complex, such as upstream pristine sediments (P1) or downstream lake sediments (G8), Zn like Cd, was bound to various fractions. In upstream pristine sediments, Zn was less concentrated than in mining impacted sediments, as would be expected in the context of mineralization (Runnels et al., 1992). The sulfide fraction (20%, Fig. 8) was the source of Zn in this sediment, presumably because at the neutral pH of the water (Table 1), sulfide alteration was slow. The neutral pH promoted adsorption of Zn onto oxides (30%), while 18% of Zn was associated with

organic matter and 20% remained in the residue, probably bound to phyllosilicates (Isaure et al., 2005). In the mining area, Zn was mostly associated with sulphide phases. Downstream, Milluni Grande Lake sediments were different compared to the pristine areas and the fresh mining wastes. The strong acidity of the lake water did not favour adsorption to this fraction (7% of Zn was bound to Fe-oxyhydroxides, Figs. 7l and 8) nor the precipitation of Mn oxides (Tessier et al., 1996). Nevertheless, a large portion of Zn (18%) was water soluble (G8) and was preferentially linked to organic matter (41%). Zinc was definitely not associated with sulfides, however, Zn content in the residual fraction remained high (30%, Fig. 7k). This suggests that just downstream of the mining sector, sphalerite has been completely altered by oxidation enhanced by AMD. The acidification process causes sustained high Zn concentrations in water, prevents adsorption onto Fe-oxyhydroxides, and results in precipitation of sulfate salts during the DS as for Cd (e.g. M9). The precipitation of sulfates such as melanterite (Fig. 7j), rozenite or copiapite (Hammarstrom et al., 2005), which are solid solutions, can include Zn (Jambor et al., 2000), and might explain the high concentration of Zn (1.2%) in M9 sediment.

4.1.3. Pb

The main mineralogical source of Pb in the sediments was galena. Under oxidizing conditions galena weathers to anglesite, which exhibits low solubility below pH 6 (Blowes et al., 2003). Galena was much less abundant than sphalerite in the Milluni Mine (Ahlfeld and Schneider-Scherbina, 1964), although some amount was brought to the mill from nearby mines (Ríos, 1985). Galena was only found in the fine sections of mine rock using optical microscopy in reflected light (not shown). The absence of galena and the presence of Pb sulfates (Fig. 7b) could be linked to the rapid alteration of galena under acid conditions (Lin and Qvarfort, 1996; Moncur et al., 2005), which was experimentally shown by Gleisner et al. (2002). This process occurs in fresh mine wastes (M10, Fig. 7b), and could explain why Pb, but not Zn, was present in all samples associated with the sulfide fraction (Fig. 8), even at the outlet of the catchment (G8). Unlike the other metals, Pb was mainly bound to OM (33%) in fresh mine waste (M10). This observation does not agree with the initial tests performed on a fresh pure galena sample, which showed that the technique was quite selective for this mineral. Moreover, even if some organic matter can be found in fresh mining wastes, it can be reasonably assumed that the OM content was negligible. This leads to the hypothesis of the presence of a major Pb-bearing mineral phase other than galena. Further investigations into the selectivity of the sequential extraction for Pb are thus needed. Indeed, the extraction step for the OM fraction uses ammonium acetate to prevent element re-adsorption (Leleyter and Probst, 1999), which was observed by Cardoso Fonseca and Martin (1986) to attack tertiary anglesite. It is thus possible that Pb might come from anglesite dissolution (Fig. 7a and b). If it is assumed that anglesite content was proportionally related to the amount of galena (1.3%), these results allow a correction coefficient (ACC) to be applied to estimate the leachable Pb sulphate during the OM extraction step.

In the upstream pristine sediments (P1), Pb partitioning seemed to be similar to that of Zn. Only 6% of Pb was associated with sulfides. Applying the ACC as a maximum value, at least 27% Pb would be bound to the OM. A rather large proportion of acid solublestage, mainly as a consequence of the presence of carbonates in the bedrock as shown by the neutral pH water conditions of this pristine granitic area (Table 1). Downstream from the mine at Milluni Grande Lake sediments (G8), applying the maximum ACC correction suggests that 43% of Pb was associated with OM. Indeed, this association of Pb with organic matter in river sediments affected by mining has previously been observed (Pagnanelli et al., 2004; Singh et al., 1998). Similarly to As, Sn and Fe (Fig. 8), the association of Pb with crystalline oxides increased from upstream to downstream, as also noticed in mineralogical observations (Table 3).

4.1.4. Fe

In pristine sediments (P1), Fe was well distributed, similarly to Pb and Zn. Neutral pH and slightly oxic conditions favoured the occurrence of sulfides and limited the precipitation of oxides. In fresh mining waste, Fe was primarily associated with the sulfide fraction, similar to other PHEs. This was probably a consequence of the relatively low weathering rate of pyrite as compared to other sulfide minerals and its abundance. Finally, downstream in Milluni Grande Lake sediments, Fe was predominantly associated with oxides (Fig. 7l), in relation to the high oxic conditions in the lake.

But it was also present in the organic fraction, probably in relation to the significant OM content (5.5%) in the lake sediments (Fig. 8).

4.1.5. Sn

Tin was virtually immobile (Fig. 8). Cassiterite dominated the residual phase, since it is a very resistant primary oxide. Only a minor fraction of Sn was found in the Fe-oxyhydroxide fraction. In fresh mining wastes, a large portion of Sn was bound to sulfides such as stannite and kesterite as also confirmed by microprobe analysis (Table 4).

4.1.6. Summary of PHE availability

Finally, with the exception of Sn, in the Milluni Valley, most PHEs were extremely mobile, as shown by sequential extractions. The general order of PHE availability in sediments was established as As > Fe > Pb > Cd > Zn ~ Cu > Sn. The maximum release was from fresh mining waste, and the minimum availability was for the sediments from the pristine granitic area (P1). Downstream in Milluni Grande Lake sediments, PHEs were highly mobile as a consequence of the intense chemical oxidation of sulfides. As a whole it could be deduced that pH played an important role in PHE availability by controlling adsorption on the different labile fractions. Only upstream of the mine did carbonates and Mn-oxides trap PHEs. Iron-oxyhydroxides significantly controlled the adsorption of PHEs, but this control was governed by the intrinsic equilibrium between the oxides and the element, which varied as a function of pH. Nevertheless, other factors, mainly OM content, played an important role in PHE complexation, as seen in Milluni Grande Lake sediments.

4.2. Lithological and mineralogical footprint on major elements and PHE composition of surface waters

The alteration products from the upper Milluni catchment were dominated by the hydrolysis of carbonates and Ca-rich silicates. In contrast, the main geochemical feature in the downstream mining area was surface water acidification, resulting from pyrite oxidation. In this basin, the Silurian bedrock possessed a low capacity to neutralize acidity originating from weathering of ore minerals.

4.2.1. Major element origins

Calcium dominated the composition of the waters draining the upper basin and those originating from the Zongo glacier, which mainly covers granitic bedrock. This is characteristic of the dissolution of calcite, which is present in veins in the granite, but also to anorthite ($CaAl_2Si_2O_8$) which is common in the study area (Table 3). No significant difference in Ca content was observed between waters draining the granitic sector (P1) and the Ordovician sandstones (P2). Indeed, Tranter (2003) indicated that in proglacial environments, waters were always Ca dominated whatever the lithology.

The waters from the intermediate sector (JK) reflect the transition between the glacial-granitic

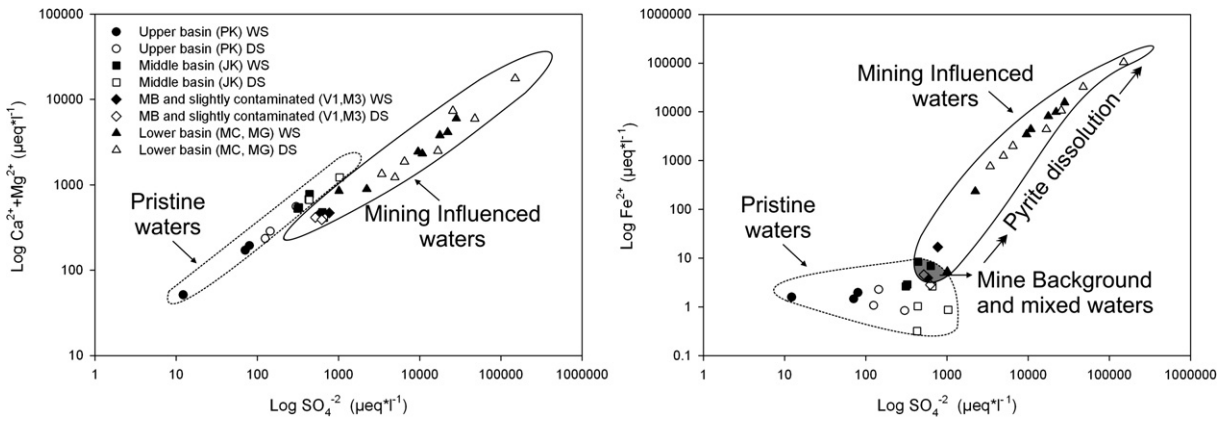

Fig. 10. log–log relationships between $Ca^{2+} + Mg^{2+}$ versus SO_4^{2-} (a), and Fe^{3+} versus SO_4^{2-} (b). Black symbols indicate wet season conditions (WS); outline symbols indicate dry season conditions (DS); PK: waters from Pata Kkota sector; JK: waters from Jankho Kkota sector; MB: water draining the background and mineralized lithology; MC: waters from Milluni Chico sector; MG: waters from Milluni Grande sector.

area and the mine area (Fig. 1). The chemical composition reveals the mixing of silicate weathering from the glacial granitic (PK) and sedimentary area, and sulphide oxidation of the mineralized geological unit.

In the Milluni Chico and Milluni Grande areas, waters were dominated by Mg and SO_4 (Fig. 3). Acidity was high (Table 1) and Fe and SO_4 were only significantly correlated ($r^2 = 0.95$, $p < 0.001$) in surface waters downstream from the mining area (Fig. 10), as a consequence of pyrite dissolution (Nordstrom et al., 1999). However, in addition to pyrite, the dissolution of other sulfides such as sphalerite, chalcopyrite and arsenopyrite produced SO_4 and acidity (Jennings et al., 2000). This acidity contributed to weathering of most soluble minerals in the sandstones (i.e. phyllosilicates, which were the main Mg^{2+} source), and explained why Mg became dominant between the pristine and mining affected waters (Fig. 3). Both in pristine and mining influenced waters, the relationship between Ca + Mg and SO_4 is positive and significant ($r^2 = 0.97$ and 0.96, $p < 0.001$, respectively, Fig. 10), whereas Fe and SO_4 were significantly related only in mining influenced waters. Therefore, pyrite dissolution was restricted in the mining contaminated waters, whereas gypsum weathering occurred in the whole valley.

4.2.2. PHE origins

The influence of mining on PHE concentrations in water has been evaluated by the calculation of an enrichment factor (EF, see Section 2.3). The general EF order in the mining impacted waters was Cd > Zn ≫ As ≫ Cu ∼ Ni > Pb > Sn. Cadmium was the most enriched element ($1 \times 10^{+3} < EF < 1 \times 10^{+5}$), consistent with its high solubility. Generally, the most enriched elements in water (Cd and Zn) were linked to the same mineral source (sphalerite). Arsenic had the next greatest EF ($2 \times 10^{+2} < EF < 4 \times 10^{+4}$), since it is a leachable element in sediments and wastes (Fig. 8, see Section 4.1.6) and it is well known to be soluble in acidic conditions during rain events in the wet season (Craw et al., 2003) as observed in Fig. 4. Zinc, Cu and Ni were highly enriched in waters downstream of the mine. Their similar enrichment (∼100) was probably due to the relative solubility of Cu and Ni in such conditions (Sigg et al., 2000), and to the mineral paragenesis. Indeed, the Cu source was primarily chalcopyrite, which was clearly associated with sphalerite (Fig. 6). Lead was only slightly enriched ($1.7 < EF < 65$) probably as a consequence of low mineral content, and due to attenuation by complexation with organic matter in sediments. With the exception of some specific sampling points surrounding the mine, and during specific hydrological conditions (Fig. 1, J8 in WS, M4 and M6 in DS), enrichment factors for Sn never exceeded 10. Thus, little Sn contamination was detected in water of the whole Milluni catchment, as it is highly insoluble (Figs. 7d and 8).

The results indicate very high concentrations of Zn and As in surface waters and a significant availability in sediment and wastes in relation to the physico-chemical conditions, which imply these two are the most dangerous pollutants in the area. Proceeding downstream, there was a very clear step in EF values (for Zn and As, Fig. 11) between pristine and slightly contaminated waters (near the background values, P1 to G9) and contaminated waters (several times the background values, M1 to G8). Three kilometers downstream from the mine (M8), the As enrichment in water ($1 \times 10^{+3} < EF < 7 \times 10^{+3}$, Fig. 11) surpassed the value of the

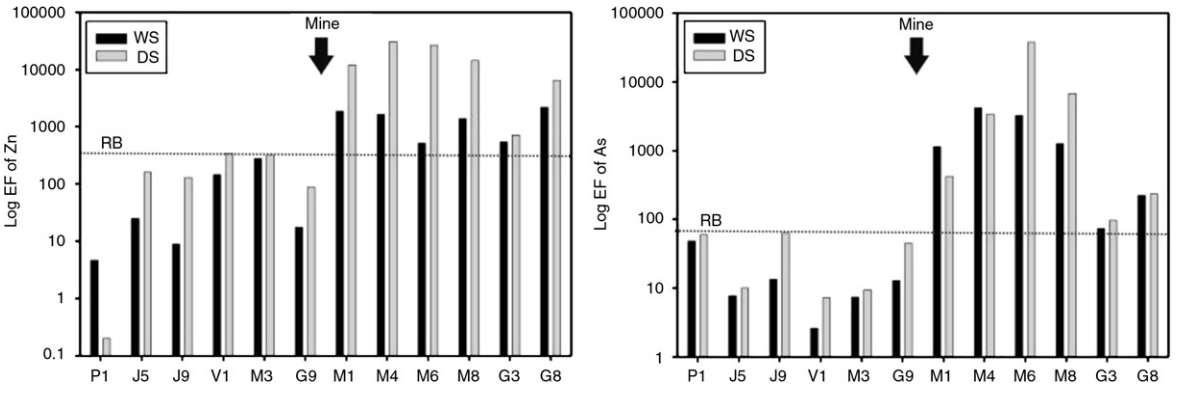

Fig. 11. Enrichment factor for Zn and As concentrations in surface waters from Milluni catchment. RB: regional background.

main mine effluent (M1), whereas EF remained high for Zn (M8 and G8, $1 \times 10^{+3} < EF < 4 \times 10^{+4}$) even 5 km downstream from the mine. At the outlet (G8), EF for both elements was lower than in the Milluni Chico sector (M1 to M8, Fig. 11), probably due to: (i) dilution of contamination by lateral tributaries of Milluni Grande Lake (with lower EF values), or (ii) attenuation by geochemical processes.

In spite of these similarities, As and Zn exhibited very distinct geochemical behaviours. A considerable decrease for As was observed at the outlet (G8, $EF < 250$), which can be explained by its adsorption onto Fe-oxyhydroxides, as demonstrated by mineralogical and chemical data (Table 3 and Fig. 8). Conversely, Zn enrichment in water might be related to the importance of the water soluble fraction in Milluni Grande Lake sediments (G8), as shown by sequential extractions (Fig. 8). Moreover, the acidic pH played a key role limiting Zn adsorption onto the sediments, and contributed to maintaining dissolved Zn in lake water.

4.3. Hydrological conditions: the role of major element and PHE transfer in surface waters

As a result of drastically lower precipitation during the winter dry season (Fig. 2), stream water discharge is greatly diminished. Less precipitation, combined with freezing, concentrated solutes in waters (higher TDS, Table 1). This effect was particularly obvious in the upper catchment and in Milluni Chico runoff and lake. This strong seasonal influence is seen in Fig. 10, where Fe and SO_4^{2-} concentrations significantly increased from WS to DS. However, SO_4 was higher than Fe_{Tot} as a consequence of (i) more conservative behaviour of SO_4 (Bencala and Ortiz, 1999), (ii) the precipitation of Fe as oxyhydroxides (Figs. 7i and 9), and (iii) the dissolution of sulfide minerals other than pyrite (e.g. sphalerite, galena).

Most PHEs in the valley are products of sulfide oxidation. With the exception of Zn in contaminated waters, higher PHE concentrations were observed in waters in the WS compared to DS (one- to three-fold, Table 2 and Figs. 2 and 4), particularly for Mn, Cu, Cd and Pb. At the beginning of the WS, rainfall recharged mine groundwaters and washed contaminated sediments leading to the dissolution of soluble minerals enriched in PHEs. This rapid dissolution contributes to the transport of elements downstream during periods of flush. This pattern was significant for As in mining effluents (M1, M4, 10 times ratio), except in the Milluni Chico sector (M6 and M8) where As, Mn, Cd and Zn concentrations were more elevated during the DS. This difference might be explained by the low slope of the area (moreover, M6 showed a very low discharge, $<0.5\ l\ s^{-1}$) and the shallow water in Milluni Chico lake (M8), which favoured water concentration by evaporation and possibly a more important contribution of concentrated sediment interstitial water to surface waters. Nevertheless, calculated loads for PHEs at the outlet of Milluni Chico sector (M8) showed that the maximum contaminant load for Pb, Cu, Cd, As and even for Zn, occurred during WS (Table 6).

Arsenic EF was higher during the DS, with the exception of the mine influents (Fig. 11). Hence there might be an apparent contradiction with the concentration pattern. This discrepancy could be related to hydrological control observed on Sc concentrations during the WS, as mentioned previously (Section 2.3). This element was mainly a dissolution product of silicates and phosphates (Barthelmy, 2005). Enhanced silicate weathering during the WS caused greater Sc concentrations, in a higher proportion than As. This was clearly seen for As EF (Fig. 11) at J9, G9 and G8.

In contrast to As, Zn concentrations as well as Zn enrichment were higher during the DS in the mine area. A negative correlation between discharge and Zn also was observed in waters from Iron Mountain in the USA (Alpers et al., 2003). The oxidation of sphalerite is not water dependent, unlike the oxidation of other sulphides. The preferential control of other PHEs by oxides and sulfate salts during the DS (Alpers et al., 2003; Craw et al., 2003) might explain their contrasting behaviour to Zn.

Table 6
Comparison of PHE loads at the oulet of Milluni Chico sector (M8) during wet (WS) and dry seasons (DS)

Point	Season	Area (km^2)	Discharge ($l\ s^{-1}$)	Metal loads ($mg\ s^{-1}\ km^{-2}$)				
				Zn	As	Pb	Cd	Cu
M8	WS	27.5	470	456	10.9	0.3	3.2	15.0
M8	DS	27.5	89.4	372	4.6	0.03	0.7	1.6

5. Conclusions

For the first time, mining related contamination in the Milluni Valley of Bolivia was investigated using a multi-disciplinary approach including geochemistry, mineralogy and hydrology. This drainage basin is the main water supply for La Paz, the capital and largest city in Bolivia. Surface water was identified as the vector for PHE transport, which can cause multiple and very serious effects on the environment, and furthermore to human health. The goal of the study was a complete characterization of PHEs in waters and sediments, the identification of sources and sinks, and the mechanisms responsible for their distribution in the environment.

Elemental concentrations were highly enriched, relative to background levels, in surface waters and sediments downstream of the Milluni Mine. As a consequence, the PHE contamination was obvious downstream from the mine, as indicated by the strongly exceeded water guideline values for human consumption. The very acidic conditions were identified as a main control on high dissolved element concentrations in surface waters. The typical order of PHE enrichment was $Cd > Zn \gg As \gg Cu \sim Ni > Pb > Sn$:

- Sulfides (sphalerite, arsenopyrite, pyrite, chalcopyrite and galena) were the primary source of Zn, Cd, As, Fe, Cu and Pb in surface water and sediments, although primary oxides were the main Sn source. Sphalerite and chalcopyrite were likely consumed by oxidation, based on their absence in the sediments at the outlet of the catchment. Arsenopyrite and mainly pyrite remain in these sediments presumably due to their lower solubility.
- The relative decrease in As contamination of surface water downstream from the mine in such acidic and oxidising conditions was related to the uptake of As by amorphous and crystalline oxides in sediments.
- Low pH in surface waters downstream of the mine favoured the high concentrations of Zn and Cd in the dissolved phase. However, climate conditions controlled the precipitation of tertiary minerals (such as melanterite) during the DS. This process was identified as a transitory element storage.
- Unexpectedly, uptake by organic matter was an important control on Zn and Pb in bottom sediments, particularly in those from Milluni Grande Lake. The exception was for sulfide-rich mining wastes, where organic matter was negligible. In the organic matter extraction step of mining waste, associated Pb was derived mainly from anglesite dissolution.
- The order of availability of PHEs in sediments was identified as follows $As > Fe > Pb > Cd > Zn \sim Cu > Sn$ according to the non-residual fractions. However, with reference to the range of water quality guideline exceedances, the order of element toxicity was $Fe > As > Cd > Zn \sim Mn > Al > Pb > Cu$ in highly contaminated waters, whereas at the outlet of the catchment it was $Fe > Cd > Zn \sim Mn > As > Al > Pb$.
- Hydrological conditions were important in modulating the element concentrations, their enrichment and loads. Contrasting behaviours were observed between major elements and PHE. During the WS, meteoric waters enhanced the mobilisation of elements from primary and unstable tertiary mineral dissolution contributing to a "flush" of contamination downstream, but dilute the concentration of major elements derived from mineral weathering.
- The study area is located in a tropical latitude with seasonally contrasted hydrological conditions, but the high altitude is responsible for a cold high mountain climate. These conditions play an important role in water contamination by mining exploitation, particularly in relation to mineral weathering and leaching processes. Hence, the geochemical behaviour of element contamination is more akin to that of temperate and cold regions than to tropical areas.
- AMD is the main source of water pollution in the area. Hence, initial remediation must focus on sealing the main mine galleries to avoid water percolation and limit acid mine drainage. This effort will mainly act to reduce the element release from mining wastes along the valley. Water in the Milluni Chico and Grande Lakes exhibits low pH; however, lake sediments represent a noteworthy sink for As via adsorption to Fe-oxyhydroxides, while Zn and Pb, to a lesser extent, are trapped by organic matter. Therefore, removal of bottom sediments would not be an appropriate remediation strategy.

Acknowledgements

Our special thanks go J.M. Montel (LMTG) for his help in XRD interpretations, F. Velasco (UPV,

University of Basque Country, Spain) for microscope reflection descriptions, O. Marsan (CIRIMAT, Toulouse) for Thermical Gravimetric analysis and the technical staff of LMTG (C. Boucayrand, F. Candaudap, J. Caparros, M. Carayon, C. Causserand, S. Gardoll, R. Freydier, T. Aigouy, P. De Parseval, F. De Parseval, J.F. Mena, C. Lagane, M. Thibaut, M. Valladon). Our gratitude also goes to the staff from IRD and the Univ. Mayor de San Andrés (Lab. Calidad del Medio Ambiente, UMSA, La Paz, Bolivia), particularly to L. Alanoca, R. Fuertes, E. Lopez and S. Sacaca, and also to the IRD Great Ice Program. The authors especially acknowledge G. Halverson (LMTG) for the English improvement of the manuscript and D. Craw, R.B. Wanty, R. Fuge and an anonymous reviewer for their helpful advice. M.M. Salvarredy-Aranguren benefited from an IRD fellowship, and financial support of the Programa Saint Exupéry (Ministerio de Educación, Ciencia y Tecnología de Rep. Argentina y Embajada de Francia en Argentina).

References

Ahlfeld, F., Schneider-Scherbina, A., 1964. Los Yacimientos Minerales y de Hidrocarburos de Bolivia. Departamento Nacional de Geología del Ministerio de Minas y Petróleo, La Paz.

Alpers, C.N., Nordstrom, D.K., Spitzley, J., 2003. Extreme acid mine drainage from a pyritic massive sulfide deposit: the Iron Mountain end-member. In: Jambor, J.L., Blowes, D.W., Ritchie, A.I.M. (Eds.), Environmental Aspects of Mine Wastes. Mineralogical Association of Canada, Vancouver, pp. 407–430.

Apaza Chavez, R., 1991. Incidencia de una contaminación por efluentes mineros sobre la fauna béntica en un complejo fluvio-lacustre andino, Milluni, La Paz, Bolivia. Tésis de grado de Biología. Universidad Mayor de San Andrés, La Paz.

Argollo, J., Gouze, P., Saliege, J.F., Servant, M., 1987. Fluctuations des glaciers de Bolivie au Quaternaire recent–late Quaternary glacial fluctuations in Bolivia. In: Martin, T.Y. (Ed.), Paleolacs et Paleoclimats en Amerique Latine et en Afrique (20 000 and B.P.-actuel) – Paleolakes and Paleoclimates in South America and Africa (20,000 years B.P.-present). Office de la Recherche Scientifique et Technique Outre-Mer (ORSTOM), Bondy, France, pp. 103–104.

Aries, S., Valladon, M., Polvé, M., Dupré, B., 2000. A routine method for oxides and hydroxide interference corrections in ICP-MS chemical analysis of environmental and geological samples. Geostand. Newslett. 24, 19–31.

Audry, S., Blanc, G., Schafer, J., 2005. The impact of sulphide oxidation on dissolved metal (Cd, Zn, Cu, Cr, Co, Ni, U) inputs into the Lot-Garonne fluvial system (France). Appl. Geochem. 20, 919–931.

Ball, J.W., Nordstrom, D.K., 1991. User's Manual for WATEQ4F, with revised thermodynamic data base and test cases for calculating speciation of major, trace, and redox elements in natural waters. In: US Geol. Surv. Open-File Rep. 91-183.

Baron, D., Palmer, C.D., 1996. Solubility of jarosite at 4–35 °C. Geochim. Cosmochim. Acta 60, 185–195.

Barthelmy, D., 2005. Mineralogy Database. <http://webmineral.com/X-Ray.shtml>.

Bencala, K.L., Ortiz, R.F., 1999. Theory and (or) reality: analysis of sulfate mass-balance at Summitville, Colorado poses process questions about the estimation of metal loadings. In: Morganwalp, D.W., Buxton, H.T. (Eds.), US Geol. Surv. Toxic Substances Hydrology Program – Technical Meeting. United States Geological Survey, Charleston, South Carolina, USA, pp. 1–16.

Bervoets, L., Solis, D., Romero, A.M., Damme, P.A.V., Ollevier, F., 1998. Trace metal levels in chironomid larvae and sediments from a Bolivian river: impact of mining activities. Ecotoxicol. Environ. Safety 41, 275–283.

Bigham, J.M., Schwertmann, U., Traina, S.J., Winland, R.L., Wolf, M., 1996. Schwertmannite and the chemical modeling of iron in acid sulfate waters. Geochim. Cosmochim. Acta 60, 2111–2121.

Blowes, D.W., Ptacek, C.J., Jambor, J.L., Weisener, C.G., 2003. The geochemistry of acid mine drainage. In: Lollar, B.S. (Ed.), Environmental Geochemistry. Treatise on Geochemistry, vol. 9. Elservier–Pergamon, Oxford, pp. 149–204.

Brunel, C., 2005, Dynamique des éléments traces métalliques (Pb, Zn et Cd) sur un petit bassin vrsant contaminé par des déchets miniers – Cas du bassin versant amont du Lez (Ariege, Pyrénees). Ph.D. Thesis, Toulouse, Univ. Paul Sabatier.

Caballero, Y., Jomelli, V., Chevallier, P., Ribstein, P., 2002. Hydrological characteristics of slope deposits in high tropical mountains (Cordillera Real, Bolivia). CATENA 47, 101–116.

Caballero, Y., Chevallier, P., Gallaire, R., Pillco, R., 2004. Flow modelling in a high mountain valley equipped with hydropower plants: Rio Zongo Valley, Cordillera Real, Bolivia. Hydrol. Process. 18, 939–957.

Callender, E., 2003. Heavy metals in the environment – historical trends. In: Lollar, B.S. (Ed.), Environmental Geochemistry. Treatise on Geochemistry, vol. 9. Elsevier–Pergamon, Oxford, pp. 67–105.

Cardoso Fonseca, E., Martin, H., 1986. The selective extraction of Pb and Zn in selected mineral and soil samples, application in geochemical exploration (Portugal). J. Geochem. Explor. 26, 231–248.

Carlson, L., Bigham, J.M., Schwertmann, U., Kyek, A., Wagner, F., 2002. Scavenging of As from acid mine drainage by schwertmannite and ferrihydrite: a comparison with synthetic analogues. Environ. Sci. Technol. 36, 1712–1719.

Carlsson, E., Thunberg, J., Ohlander, B., Holmstrom, H., 2002. Sequential extraction of sulfide-rich tailings remediated by the application of till cover, Kristineberg mine, northern Sweden. Sci. Total Environ. 299, 207–226.

Chatelain, D., Wittinton, H.M., 1992. Evaluación de los Recursos Hídricos en Bolivia, Sur América. In: Ricaldi, V., Flores, C., Anaya, L. (Eds.), Seminario de los Recursos Hídricos en Bolivia y su Dimensión Ambiental. Cochabamba, pp. 133–136.

Cornell, R., Schwertmann, U., 1996. The Iron Oxides, Structures, Properties, Reactions, Occurence and Uses. Wiley–VCH Verlag GMBH & Co., KGaA.

Courtin-Nomade, A., Bril, H., Neel, C., Lenain, J.-F., 2003. Arsenic in iron cements developed within tailings of a former metalliferous mine – Enguiales, Aveyron, France. Appl. Geochem. 18, 395–408.

Craw, D., Falconer, D., Youngson, J.H., 2003. Environmental arsenopyrite stability and dissolution: theory, experiment, and field observations. Chem. Geol. 199, 71–82.

Crespo, L.S., 1936. La ciudad de La Paz. Rev. Geogr. Am. 28, 61–66.

Dittmar, T., 2004. Hydrochemical processes controlling arsenic and heavy metal contamination in the Elqui river system (Chile). Sci. Total Environ. 325, 193–207.

Dold, B., 2003. Speciation of the most soluble phases in a sequential extraction procedure adapted for geochemical studies of copper sulfide mine waste. J. Geochem. Explor. 80, 55–68.

Dold, B., Fontbote, L., 2002. A mineralogical and geochemical study of element mobility in sulfide mine tailings of Fe oxide Cu–Au deposits from the Punta del Cobre belt, northern Chile. Chem. Geol. 189, 135–163.

Espi, E., Boutron, C.F., Hong, S., Pourchet, M., Ferrari, C., Shotyk, W., Charlet, L., 1997. Changing concentrations of Cu, Zn, Cd and Pb in a high altitude peat bog from Bolivia during the past three centuries. Water Air Soil Pollut. 100, 289–296.

Fanfani, L., Zuddas, P., Chessa, A., 1997. Heavy metals speciation analysis as a tool for studying mine tailings weathering. J. Geochem. Explor. 58, 241–248.

Fernández, S., Thompson, C., 1995. Hoja 5945 Milluni (1:100,000). Serie I-CGB-34. Servicio Geológico de Bolivia, La Paz.

Ferrari, C.P., Clotteau, T., Thompson, L.G., Barbante, C., Cozzi, G., Cescon, P., Hong, S., Maurice-Bourgoin, L., Francou, B., Boutron, C.F., 2001. Heavy metals in ancient tropical ice: initial results. Atmos. Environ. 35, 5809–5815.

Filgueiras, A.V., Lavilla, I., Bendicho, C., 2002. Chemical sequential extraction for metal partitioning in environmental solid samples. J. Environ. Monitor. 4, 823–857.

Filippi, M., 2004. Oxidation of the arsenic-rich concentrate at the Prebuz abandoned mine (Erzgebirge Mts., CZ): mineralogical evolution. Sci. Total Environ. 322, 271–282.

Galay Burgos, M., Rainbow, P.S., 2001. Availability of cadmium and zinc from sewage sludge to the flounder, Platichthys flesus, via a marine food chain. Mar. Environ. Res. 51, 417–439.

Galeano, E., 1971. Las venas abiertas de América Latina. Siglo XXI de España Editores.

Garcia-Sanchez, A., Alvarez-Ayuso, E., 2003. Arsenic in soils and waters and its relation to geology and mining activities (Salamanca Province, Spain). J. Geochem. Explor. 80, 69–79.

Gasharova, B., Gottlicher, J., Becker, U., 2005. Dissolution at the surface of jarosite: an *in situ* AFM study. Chem. Geol. 215, 499–516.

Gleisner, M., Herbert, J., Roger, B., 2002. Sulfide mineral oxidation in freshly processed tailings: batch experiments. J. Geochem. Explor. 76, 139–153.

Gomez Ariza, J.L., Giraldez, I., Sanchez-Rodas, D., Morales, E., 2000. Metal sequential extraction procedure optimized for heavily polluted and iron oxide rich sediments. Anal. Chim. Acta 414, 151–164.

Gray, N.F., 1997. Environmental impact and remediation of acid mine drainage: a management problem. Environ. Geol. 30, 62–71.

Hammarstrom, J.M., Seal II, R.R., Meier, A.L., Kornfeld, J.M., 2005. Secondary sulfate minerals associated with acid drainage in the eastern US: recycling of metals and acidity in surficial environments. Chem. Geol. 215, 407–431.

Hernandez, L.M., 2003, Dynamique des éléments traces métalliques dans les sols de différents écosystèmes français. Ph.D. Thesis, Toulouse, Univ. Paul Sabatier.

Hernandez, L., Probst, A., Probst, J.L., Ulrich, E., 2003. Heavy metal distribution in some French forest soils: evidence for atmospheric contamination. Sci. Total Environ. 312, 195–219.

Hudson-Edwards, K.A., Macklin, M.G., Miller, J.R., Lechler, P.J., 2001. Sources, distribution and storage of heavy metals in the Rio Pilcomayo, Bolivia. J. Geochem. Explor. 72, 229–250.

Hudson Edwards, K.A., Miller, J.R., Preston, D., Lechler, P.J., Macklin, M.G., Miners, J.S., Turner, J.N., 2003. Effects of heavy metal pollution in the Pilcomayo river system, Bolivia, on resident human populations. J. Phys. IV 107, 637–640.

Ingersoll, C.G., MacDonald, D.D., Wang, N., Crane, J.L., Field, L.J., Haverland, P.S., Kemble, N.E., Lindskoog, R.A., Severn, C., Smorong, D.E., 2000. Prediction of Sediment Toxicity using Consensus-based Freshwater Sediment Quality Guidelines. US Environmental Protection Agency (USEPA), Chicago.

Isaure, M.-P., Manceau, A., Geoffroy, N., Laboudigue, A., Tamura, N., Marcus, M.A., 2005. Zinc mobility and speciation in soil covered by contaminated dredged sediment using micrometer-scale and bulk-averaging X-ray fluorescence, absorption and diffraction techniques. Geochim. Cosmochim. Acta 69, 1173–1198.

Jambor, J.L., Nordstrom, D.K., Alpers, C.N., 2000. Metal-sulfate salts from sulfide mineral oxidation. In: Alpers, C.N., Jambor, J.L., Nordstrom, D.K. (Eds.), Sulfate Mineral, Crystallography, Geochemistry and Environmental Significance. Mineralogical Society of America, Virginia, pp. 303–350.

Jennings, S.R., Dollhopf, D.J., Inskeep, W.P., 2000. Acid production from sulfide minerals using hydrogen peroxide weathering. Appl. Geochem. 15, 247–255.

Lehmann, B., 1978. Memoria explicativa del mapa geológico de Milluni, Cordillera Real (Bolivia). Revista de Geociencias, Universidad Mayor de San Andrés 2, 187–257.

Leleyter, L., Probst, J.-L., 1999. A new sequential extraction procedure for the speciation of particulate trace elements in river sediments. Int. J. Environ. Anal. Chem. 73, 109–128.

Leleyter, L., Probst, J.-L., Depetris, P., Haida, S., Mortatti, J., Rouault, R., Samuel, J., 1999. REE distribution pattern in river sediments: partitioning into residual and labile fractions. Comp. Rend. de l'Acad. Sci. Ser. IIA: Earth Planet. Sci. 329, 45–52.

Licheng, Z., Guijiu, Z., 1996. The species and geochemical characteristics of heavy metals in the sediments of Kangjiaxi River in the Shuikoushan Mine area, China. Appl. Geochem. 11, 217–222.

Lin, Z., Qvarfort, U., 1996. Predicting the mobility of Zn, Fe, Cu, Pb, Cd from roasted sulfide (pyrite) residues – a case study of wastes from the sulfuric acid industry in Sweden. Waste Manage. 16, 671–681.

Lodenius, M., Malm, O., 1998. Mercury in the Amazon. Rev. Environ. Contam. Toxicol. 157, 25–52.

Maurice-Bourgoin, L., Alanoca, L., Fraizy, P., Vauchel, P., 2003. Sources of mercury in surface waters of the upper Madeira erosive basins, Bolivia. J. Phys. IV 107, 855–858.

Meneses-Quisbert, R.I., 1997. Estudio de la Vegetación en la Zona Minera de Milluni, Provincia de Murillo, Departamento La Paz. Universidad Mayor de San Andrés, La Paz.

Miller, J.R., Hudson-Edwards, K.A., Lechler, P.J., Preston, D., Macklin, M.G., 2004. Heavy metal contamination of water, soil and produce within riverine communities of the Rio Pilcomayo basin, Bolivia. Sci. Total Environ. 320, 189–209.

Moncur, M.C., Ptacek, C.J., Blowes, D.W., Jambor, J.L., 2005. Release, transport and attenuation of metals from an old tailings impoundment. Appl. Geochem. 20, 639–659.

Montes de Oca, I., 1982. Geografía y Recursos Naturales de Bolivia. Bancos Central de Bolivia y Cochabamba, La Paz.

Morillo, J., Usero, J., Gracia, I., 2002. Partitioning of metals in sediments from the Odiel River (Spain). Environ. Int. 28, 263–271.

Muller, B., Axelsson, M.D., Ohlander, B., 2002. Adsorption of trace elements on pyrite surfaces in sulfidic mine tailings from Kristineberg (Sweden) a few years after remediation. Sci. Total Environ. 298, 1–16.

National Laboratory for Environmental Testing, 2002. Certified Reference Materials and Quality Assurance Services. Catalogue v 5.2. National Water Research Institute.

Nordstrom, D.K., Alpers, C.N., 1999. Negative pH, efflorescent mineralogy, and consequences for environmental restoration at the Iron Mountain Superfund site, California. Proc. Natl. Acad. Sci. USA 96, 3455–3462.

Nordstrom, D.K., Alpers, C.N., Coston, J.A., Taylor, H.E., McCleskey, R.B., Ball, J.W., Ogle, S., Cotsifas, J.S., Davis, J.A., 1999. Geochemistry, toxicity, and sorption properties of contaminated sediments and pore waters from two reservoirs receiving acid mine drainage. In: Proceedings of the Technical Meeting Charleston South Carolina, pp. 289–296.

Nriagu, J.O., 1996. A history of global metal pollution. Science 272, 223.

Oporto, C., Vandecasteele, C., Smolders, E., 2007. Elevated cadmium concentrations in potato tubers due to irrigation with river water contaminated by mining in Potosi, Bolivia. J. Environ. Qual. 36, 1181–1186.

O.P.S., 1987. Guías para la Calidad del Agua Potable. Criterios Relativos a la Salud y otra Información de Base. Organización Panamericana de la Salud, Washington.

Oyarzun, R., Lillo, J., Higueras, P., Oyarzun, J., Maturana, H., 2004. Strong arsenic enrichment in sediments from the Elqui watershed, Northern Chile: industrial (gold mining at El Indio-Tambo district) vs. geologic processes. J. Geochem. Explor. 84, 53–64.

Pagnanelli, F., Moscardini, E., Giuliano, V., Toro, L., 2004. Sequential extraction of heavy metals in river sediments of an abandoned pyrite mining area: pollution detection and affinity series. Environ. Pollut. 132, 189–201.

Perez, H., Esktrom, T., 1995. Hoja 5944 La Paz. Serie I-CGB-35. Servicio Geológico de Bolivia, La Paz.

Pfeiffer, W.C., Lacerda, L.D., Salomons, W., Malm, O., 1993. Environmental fate of mercury from gold mining in the Brazilian Amazon. Environ. Rev. 1, 26–37.

Plant, J.A., Klaver, G., Locutura, J., Salminen, R., Vrana, K., Fordyce, F.M., 1997. The forum of European Geological Surveys Geochemistry Task Group inventory 1994–1996. J. Geochem. Explor. 59, 123–146.

Ribstein, P., Tiriau, E., Francou, B., Saravia, R., 1995. Tropical climate and glacier hydrology: a case study in Bolivia. J. Hydrol. 165, 221–234.

Rimstidt, J.D., Vaughan, D.J., 2003. Pyrite oxidation: a state-of-the-art assessment of the reaction mechanism. Geochim. Cosmochim. Acta 67, 873–880.

Ríos, C.G., 1985. Estudio de la Contaminación Ambiental por las Descargas Mineras de COMSUR en la Represa de Milluni. Universidad Mayor de San Andrés, La Paz.

Romero, L., Alonso, H., Campano, P., Fanfani, L., Cidu, R., Dadea, C., Keegan, T., Thornton, I., Farago, M., 2003. Arsenic enrichment in waters and sediments of the Rio Loa (Second Region, Chile). Appl. Geochem. 18, 1399–1416.

Runnels, D.D., Sheperd, T.A., Angino, E.E., 1992. Metals in water, determining natural background concentrations in mineralized areas. Environ. Sci. Technol. 26, 2316–2323.

Sanchez España, J., Lopez Pamo, E., Santofimia, E., Aduvire, O., Reyes, J., Barettino, D., 2005. Acid mine drainage in the Iberian Pyrite Belt (Odiel river watershed, Huelva, SW Spain): geochemistry, mineralogy and environmental implications. Appl. Geochem. 20, 1320–1356.

Savage, K.S., Bird, D.K., O'Day, P.A., 2005. Arsenic speciation in synthetic jarosite. Chem. Geol. 215, 473–498.

Schippers, A., Jozsa, P., Sand, W., 1996. Sulfur chemistry in bacterial leaching of pyrite. Appl. Environ. Microbiol. 62, 3424–3431.

Schütz, L., Rahn, K.A., 1982. Trace elements concentration in erodeable soils. Atmos. Environ. 16, 171–176.

Seal, R.R., Hammarstrom, J.M., 2003. Geoenvironmental models of minerals deposits: examples from massive sulfides and gold deposits. In: Jambor, J.L., Blowes, D.W., Ritchie, A.I.M. (Eds.), Environmental Aspects of Mine Wastes. Mineralogical Association of Canada, Ottawa, pp. 11–50.

Shotyk, W., 1996. Peat bog archives of atmospheric metal deposition: geochemical evaluation of peat profiles, natural variations in metal concentrations, and metal enrichment factors. Environ. Rev. 4, 149–183.

Sigg, L., Behra, P., Stumm, W., 2000. Chimie des Milieux Aquatiques. Dunod, Paris.

Singh, S.P., Tack, F.M., Verloo, M.G., 1998. Heavy metal fractionation and extractability in dredged sediment derived surface soils. Water Air Soil Pollut. 102, 313–328.

Smedley, P.L., Kinniburgh, D.G., 2002. A review of the source, behaviour and distribution of arsenic in natural waters. Appl. Geochem. 17, 517–568.

Smichowski, P., Polla, G., Gomez, D., 2005. Metal fractionation of atmospheric aerosols via sequential chemical extraction: a review. Anal. Bioanal. Chem. 381, 302–316.

Smolders, A.J.P., Hudson-Edwards, K.A., Van der Velde, G., Roelofs, J.G.M., 2004. Controls on water chemistry of the Pilcomayo River (Bolivia, South-America). Appl. Geochem. 19, 1745–1758.

Sondag, F., 1981. Selective extraction procedures applied to geochemical prospecting in an area contaminated by old mine workings. J. Geochem. Explor. 15, 645–652.

Tessier, A., Fortin, D., Belzile, N., DeVitre, R.R., Leppard, G.G., 1996. Metal sorption to diagenetic iron and manganese oxyhydroxides and associated organic matter: narrowing the gap between field and laboratory measurements. Geochim. Cosmochim. Acta 60, 387–404.

Tranter, M., 2003. Geochemical weathering in glacial and proglacial environments. In: Drever, J.I. (Ed.), Surface and Ground Water, Weathering, and Soils. Treatise on Geochemistry, vol. 5. Elsevier–Pergamon, Oxford, pp. 189–206.

Wagnon, P., Ribstein, P., Kaser, G., Berton, P., 1999. Energy balance and runoff seasonality of a Bolivian glacier. Global Planet. Change 22, 49–58.

Wasserman, J.C., Hacon, S., Wasserman, M.A., 2003. Biogeochemistry of mercury in the Amazonian environment. AMBIO 32, 336–342.

Wedepohl, H.K., 1995. The composition of the continental crust. Geochim. Cosmochim. Acta 59, 1217–1232.